The Plant Cell, Vol. 14, 387–406, February 2002, www.plantcell.org © 2002 American Society of Plant Biologists

The Abscisic Acid–Related SNARE Homolog NtSyr1 Contributes to Secretion and Growth: Evidence from Competition with Its Cytosolic Domain

Danny Geelen,[a,1,2] Barbara Leyman,[a,1,3] Henri Batoko,[b] Gian-Pietro Di Sansabastiano,[a] Ian Moore,[b] and Michael R. Blatt[a,4,5]

[a] Laboratory of Plant Physiology and Biophysics, Imperial College of Science, Technology, and Medicine at Wye, Kent TN25 5AH, United Kingdom

[b] Department of Plant Sciences, University of Oxford, South Parks Road, Oxford OX1 3RB, United Kingdom

Syntaxins and other SNARE proteins are crucial for intracellular vesicle trafficking, fusion, and secretion. Previously, we isolated the syntaxin-related protein NtSyr1 (NtSyp121) from tobacco in a screen for abscisic acid–related signaling elements, demonstrating its role in determining the abscisic acid sensitivity of K^+ and Cl^- channels in stomatal guard cells. NtSyr1 is localized to the plasma membrane and is expressed normally throughout the plant, especially in root tissues, suggesting that it might contribute to cellular homeostasis as well as to signaling. To explore its functions in vivo further, we examined stably transformed lines of tobacco that expressed various constructs of *NtSyr1*, including the full-length protein and a truncated fragment, Sp2, corresponding to the cytosolic domain shown previously to be active in suppressing ion channel response to abscisic acid. Constitutively overexpressing NtSyr1 yielded uniformly high levels of protein (>10 times the wild-type levels) and was associated with a significant enhancement of root growth in seedlings but not with any obvious phenotype in mature, well-watered plants. Similar transformations with constructs encoding the Sp2 fragment of NtSyr1 showed altered leaf morphology but gave only low levels of Sp2 fragment, suggesting a strong selective pressure against plants expressing this protein. High expression of the Sp2 fragment was achieved in stable transformants under the control of a dexamethasone-inducible promoter. Sp2 expression was correlated positively with altered cellular and tissue morphology in leaves and roots and with a cessation of growth in seedlings. Overexpression of the full-length NtSyr1 protein rescued the wild-type phenotype, even in plants expressing high levels of the Sp2 fragment, supporting the idea that the Sp2 fragment interfered specifically with NtSyr1 function by competing with NtSyr1 for its binding partners. To explore NtSyr1 function in secretion, we used a green fluorescent protein (GFP)–based section assay. When a secreted GFP marker was coexpressed with Sp2 in tobacco leaves, GFP fluorescence was retained in cytosolic reticulate and punctate structures. In contrast, in plants coexpressing secreted GFP and NtSyr1 or secreted GFP alone, no GFP fluorescence accumulated within the cells. A new yellow fluorescent protein–based secretion marker was used to show that the punctate structures labeled in the presence of Sp2 colocalized with a Golgi marker. These structures were not labeled in the presence of a dominant Rab1 mutant that inhibited transport from the endoplasmic reticulum to the Golgi. We propose that NtSyr1 functions as an element in SNARE-mediated vesicle trafficking to the plasma membrane and is required for cellular growth and homeostasis.

INTRODUCTION

Membrane trafficking to and from the plasma membrane in all eukaryotic cells is mediated by exocytotic and endocytotic fusion of vesicles from endosomal compartments. These processes sustain membrane protein turnover and

[1] These authors contributed equally to this work.

[2] Current address: Laboratorium voor Genetica, Departement Planten Genetica, Vlaams Interuniversitair Instituut voor Biotechnologie, Universiteit Gent, K.L. Ledeganckstraat 35, B-9000 Gent, Belgium.

[3] Current address: Laboratorium Molecular Cell Biology, Institute of Botany and Microbiology, Department of Biology, Katholieke Universiteit Leuven, Kardinaal Mercierlaan 92, B-3001 Leuven-Heverlee, Belgium.

[4] Current address: Laboratory of Plant Physiology and Biophysics, Institute Of Biomedical and Life Sciences, Bower Building, University of Glasgow, Glasgow G128QQ, UK.

[5] To whom correspondence should be addressed. E-mail m.blatt @bio.gla.ac.uk; fax 44-0-141-330-4447.

Article, publication date, and citation information can be found at www.plantcell.org/cgi/doi/10.1105/tpc.010328.

thereby contribute to cellular homeostasis, differentiation, and growth. In plants, as in mammalian tissues, exocytotic and endocytotic events have been identified with stepwise changes in capacitance that accompany the increase or decrease of membrane surface area during vesicle membrane fusion and removal, respectively (Battey et al., 1996; Thiel and Battey, 1998). Factors affecting vesicle traffic in several instances have been shown to include cytosol-free Ca^{2+} concentration ($[Ca^{2+}]_i$) and guanosine nucleotides (Homann and Tester, 1997; Carroll et al., 1998). Furthermore, the discovery of separate $[Ca^{2+}]_i$-dependent and $[Ca^{2+}]_i$-independent pathways leading to exocytosis has underscored the subtlety of secretory processing that must occur through different mechanisms in a single cell type (Homann and Tester, 1997; Sutter et al., 2000). These kinetic and physiological details aside, there is still a paucity of information on the molecular elements that mediate secretion in plants (Battey and Blackbourn, 1993; Blatt et al., 1999).

Central to the process of vesicle fusion is a family of membrane trafficking proteins called SNAREs (for soluble NSF [*N*-ethylmaleimide–sensitive factor] attachment protein receptors) that are conserved from yeast to mammals (Bennett et al., 1993; Kaiser et al., 1997; Nichols and Pelham, 1998; Jahn and Sudhof, 1999). Complementary SNAREs are localized to different membrane compartments and therefore are thought to contribute significantly to the specificity of membrane recognition. Interactions between the vesicle and the target membrane lead to the formation of a complex of target membrane–associated SNAREs (t-SNAREs; in nerve, syntaxin, and SNAP25) and vesicle membrane–associated SNAREs (v-SNAREs; in nerve, syntaptobrevin, or vesicle-associated membrane protein). In reconstituted membrane preparations, this heterotrimeric complex comprises a minimal set of proteins required for fusion (Weber et al., 1998; Nickel et al., 1999; Parlati et al., 1999). However, in most cases, other cytoplasmic factors—including the *N*-ethylmaleimide–sensitive factor, Sec1 and its homologs—bind either before or during the formation of this SNARE complex to control and facilitate interaction between the SNARE elements and fusion (Jahn and Sudhof, 1999; Misura et al., 2000).

Syntaxins are the best characterized SNAREs and are central to the coordination of exocytosis. The large number of mammalian syntaxins, and their distribution between and within cell types, indicates a degree of specialization that parallels the numbers of vesicle targets in vivo. Nonetheless, significant overlaps in function and cellular distribution also are evident. The yeast syntaxin Sed5p, for example, interacts with at least three v-SNAREs and mediates vesicle traffic both to and from the Golgi apparatus (Nichols and Pelham, 1998), whereas the syntaxins Sso1p and Sso2p colocalize to the plasma membrane and appear to serve redundant functions in secretion (Aalto et al., 1993). In plants, the different syntaxin genes almost certainly far outnumber the identifiable membrane compartments (Blatt et al., 1999). Relatively little detail is available in most cases, but there is some evidence to suggest an associated functional diversity. The Arabidopsis syntaxins AtPep12 and AtVam3 may be identified with distinct subpopulations of prevacuolar and vacuolar compartments (Conceicao et al., 1997; Sato et al., 1997; Sanderfoot et al., 1999; Zheng et al., 1999), and the Knolle syntaxin is found only in dividing cells closely allied with the phragmoplast (Lukowitz et al., 1996; Lauber et al., 1997). Thus, plants may associate a high degree of specialization with these SNAREs, possibly coupling their actions to novel functions that have no counterpart in other organisms.

Previously, we identified a syntaxin-related protein from tobacco, NtSyr1 (NtSyp121) (Sanderfoot et al., 2000), with a role in abscisic acid responses in guard cells (Leyman et al., 1999). NtSyr1 was cleaved by the *Clostridium* neurotoxin BotN/C, and both the neurotoxin and the cytosolic (so-called Sp2) domain of NtSyr1 blocked K^+ and Cl^- channel responses to abscisic acid in vivo when loaded in guard cells. NtSyr1 is localized to the plasma membrane, and although originally cloned from a leaf cDNA library, the protein is expressed throughout the plant (Leyman et al., 2000). To gain further insight into NtSyr1 function in the whole plant, we transformed tobacco to overexpress the full-length NtSyr1 protein and its soluble Sp2 fragment. Stable expression of the full-length protein was associated with a significant, if small, increase in growth rate but otherwise had no overt effect on plant development. In contrast, plants expressing the Sp2 fragment showed stunting, altered leaf morphology, and a cessation of root growth. Expression of Sp2 inhibited secretion of a green fluorescent protein (GFP) marker. Furthermore, the effects of Sp2 on secretion and root growth could be suppressed by enhanced expression of NtSyr1. These results are consistent with NtSyr1 function in vesicle trafficking, and they suggest a more general requirement for the protein in cellular growth and homeostasis, in addition to its role in abscisic acid signaling.

RESULTS

Stable Transformation with the NtSyr1 Cytosolic Fragment Is Facilitated by Expression under an Inducible Promoter

Initially, we cloned the entire *NtSYR1* gene downstream of the 35S promoter of cauliflower mosaic virus in the binary plasmid vector pSLJ75516 (Jones et al., 1992) for *Agrobacterium tumefaciens*–mediated transformation. Subsequently, we cloned *NtSyr1* and the coding sequence for the first 279 amino acids—thus lacking the C-terminal membrane anchor (Sp2)—downstream of the 35S promoter in the pCAMBIA1380 binary vector to include an N-terminal RGS-His_6 tag. The resulting constructs, designated *Sp1*, *HSp1*, and *HSp2*, were used in tobacco leaf disc transformations, and candidate lines were analyzed for protein expression using purified anti-Sp2 antibodies (Leyman et al., 1999) after selection for growth on 50 mg/L d,l-phorphothricin (PPT) (pSLJ5516) or 50 mg/L hygromycin (pCAMBIA1380). From *Sp1* and *HSp1* transformations, >50 independent lines were isolated. Twenty lines were selected in each case for detailed analysis. Transformations with *HSp2* yielded 29 independent lines, all of which were characterized.

Figures 1A and 1B show protein gel blots from two lines each expressing either *HSp1* or *HSp2*. Primary analysis of the *Sp1* transgenic lines is summarized elsewhere (Leyman et al., 2000). The HSp1 product showed an apparent molecular mass of 34 kD on PAGE and comigrated with native NtSyr1. The anti-Sp2 antibody also detected a second protein band near 32 kD, evident as a faint band below the major band in Figure 1A. Because the *NtSyr1* gene includes a second, in-frame start codon 25 amino acid residues downstream, this protein could be the alternative translation product (predicted molecular mass, 33.8 kD). However, we cannot exclude partial degradation of HSp1. In all 20 lines, HSp1 was uniformly abundant, estimated to be ~20-fold the level of NtSyr1 in wild-type (nontransformed) tobacco and tobacco transformed with the empty vector cassette only (data not shown). Similar results were obtained from the *Sp1* transgenic lines (data not shown; see Leyman et al., 2000). The HSp1 protein also was detected when reprobed with a His_6 monoclonal antibody, confirming the identity of the protein band (Figure 1A). In contrast, tobacco transformed with the *HSp2* construct was not uniform in its expression. The predicted HSp2 peptide is 21 amino acid residues shorter than Sp1 and, on SDS-PAGE, migrated together with Sp2 purified from recombinant *Escherichia coli* cultures (Figure 1B). However, only eight of the 29 *HSp2*-transformed lines showed a measurable product on protein gel blot analysis (Figure 1B). The expression level of the native NtSyr1 protein was unaffected by the expression of HSp2 (Figure 1B and data not shown).

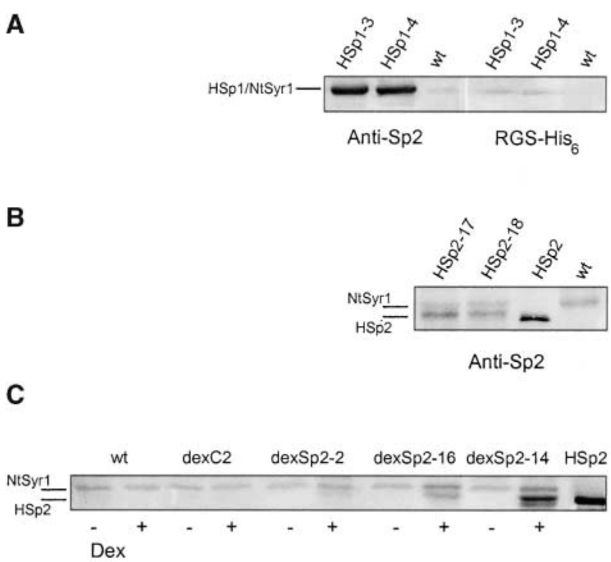

Figure 1. Expression of NtSyr1 and Related Peptide Constructs in Transformed Tobacco.

Protein gel blot analysis of SDS-PAGE with total protein extracts from 14-day-old seedlings grown on MS medium. Lanes loaded with 10 μg of total protein and probed with anti-Sp2 antibody (Leyman et al., 1999) or RGS-His_6 monoclonal antibody (see Methods).

(A) Protein from *HSp1-3* and *HSp1-4* transgenic lines and wild-type (wt) tobacco probed first with anti-Sp2 and subsequently with RGS-His_6 antibody.

(B) Protein from *HSp2-17* and *HSp2-18* transgenic lines, wild-type (wt) tobacco, and HSp2 protein purified from *E. coli* (Leyman et al., 1999) probed with anti-Sp2 antibody.

(C) Protein from wild-type (wt) tobacco and transgenic tobacco lines *dexC2* (empty vector control), *dexSp2-2*, *dexSp2-16*, and *dexSp2-14* grown either in the absence (−) or presence (+) of 1 μM dexamethasone (Dex) and probed with anti-Sp2 antibody. The far right lane was loaded with purified HSp2.

The low levels of protein recovered from these plants and, generally, the difficulty in recovering the *HSp2*-transformed plants led us to suspect that expression of the truncated NtSyr1 fragment had adverse effects on tissue viability. With the possibility of toxic effects of the Sp2 peptide in mind, we also subcloned the *Sp2* construct to bring its expression under the control of the pTA7002 dexamethasone-inducible promoter (Aoyama and Chua, 1997). Thirteen independent lines were recovered for analysis after transformations with this *dexSp2* construct. Five lines were isolated after transformation with the empty pTA7002 vector alone (*dexC*). Of the *dexSp2* lines, five expressed the Sp2 peptide strongly in the presence of dexamethasone, four lines showed an intermediate level of expression, and four showed weak expression of the peptide (Figure 1C; see also Figure 5). In each case, protein gel blots with the anti-Sp2 antibody detected two protein bands at 28 and 30 kD. These molecular masses closely match those of the translation products (28.8 and 31.5 kD) predicted from the two start codons that yield alternative Sp2 polypeptides of 254 and 278 amino acids (see above). For the sake of simplicity, we refer to both peptides as Sp2 throughout this article. As expected, the Sp2 product was soluble. NtSyr1, like other syntaxins, includes a single membrane-spanning domain at its C terminus and was found previously to copurify with the plasma membrane from tobacco leaves (Leyman et al., 2000). The Sp2 product lacks this domain, and its expression resulted in the anti-Sp2 epitope appearing in the supernatant after ultracentrifugation (Leyman et al., 1999, 2000).

Induction of the *dexSp2* transgene was characterized in seedlings grown in liquid cultures. Measurable Sp2 product was found 1 hr after adding 10 μM dexamethasone, and a steady state was achieved within 12 hr of the addition (Figure 2A). Sp2 protein levels remained stationary thereafter in the presence of dexamethasone. Concentrations of dexamethasone as low as 0.1 μM were sufficient to induce Sp2 production at near maximal levels (Figure 2B). Higher

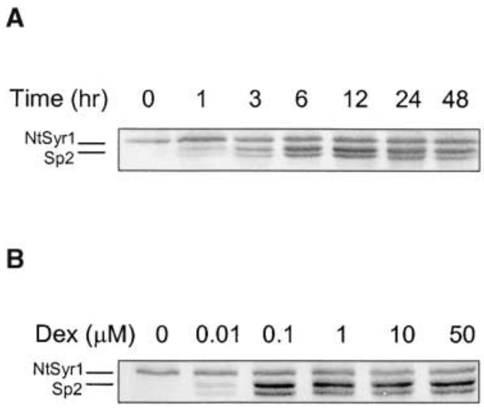

Figure 2. Kinetics of Sp2 Peptide Accumulation on Induction by Dexamethasone.

Protein gel blot analysis of total protein (10 μg/lane) from seedlings of *dexSp2-14* transgenic tobacco. Blots were probed with anti-Sp2 antiserum.

(A) Time course of Sp2 induction after treatment with 10 μM dexamethasone.

(B) Dependence of expression on dexamethasone (Dex) concentration. Plants were harvested 12 hr after dexamethasone treatment. The native NtSyr1 and the Sp2 doublet are indicated at left.

concentrations did not accelerate the time course for induction, and virtually identical kinetics were observed in the strong, intermediate, and weak expressing lines (data not shown). In the absence of dexamethasone, Sp2 remained undetected (Figures 1B and 2). Similar kinetics of gene expression have been observed in Arabidopsis transformed with the *avRpt2* gene under the control of the same promoter cassette (McNellis et al., 1998).

Sp2, but Not Sp1, Expression Alters Leaf Development

Sp1 and *HSp1* transgenic tobacco showed vigorous growth in the glasshouse, with leaf and floral morphologies indistinguishable from those of the wild type and vector controls. Indeed, germinating *Sp1*- and *HSp1*-transgenic tobacco showed a significant growth advantage over the controls (see below). In contrast, 6 of the 29 transgenic lines carrying the *Sp2* construct under the control of the 35S promoter showed some alterations in leaf development compared with controls grown side by side in the glasshouse. In each case, young leaves were chlorotic, greening late and only as the blade expanded fully (Figure 3). The leaf edges curled toward the adaxial side and along the axis of the central vein and, when fully expanded, retained a wrinkled edge with areas of small depressions and irregular deformations over the surface of the blade. Morphometric analysis indicated a reduced expansion of the mature leaf blade in these *Sp2* transgenic plants to give a lanceolate form. The mean ratio of leaf width to length in the fully expanded leaves was 0.65 ± 0.03 (n = 10 plants) for the wild type and 0.44 ± 0.05 (n = 12, pooled 2 from each line) for the *Sp2* transgenic plants, although the overall length of the leaves was not significantly different. Protein gel blot analysis (data not shown) confirmed that Sp2 expression was highest in the most affected leaves and plants.

Plants with approximately five- to 10-fold higher levels of Sp2 expression were recovered among the *dexSp2* transgenic plants compared with *Sp2* transgenic plants (Figures 1 and 2). In the absence of dexamethasone, all *dexSp2* transgenic plants were indistinguishable from the wild type. Spraying daily with 20 μM dexamethasone led to alterations in leaf morphology similar to those of the *Sp2* transgenic plants, albeit of greater severity (Figure 3). A paling and chlorosis was evident, even in young mature leaves, and especially in areas removed from vascular tissue and with longer exposures of 5 to 7 days, distortions in leaf shape were evident. The edges of the leaves curled, and the lamina bulged irregularly in and out of the surface of the blade. These leaves were unusually turgid and thus particularly sensitive to mechanical damage. Wild-type and vector control plants and *Sp1* transgenic lines also were treated with dexamethasone in parallel, but they showed normal leaf morphology and development similar to that observed for wild-type plants without dexamethasone (Figure 3). In cross-section, mature leaves of dexamethasone-treated *dexSp2* transgenic plants showed an irregular mosaic of hypertrophic cells, a much-expanded thickness to the laminae, and irregular loss of organization between palisade and spongy mesophyll (Figure 4). Such characteristics were never observed in *Sp1* transgenic, vector control, or wild-type plants, either with or without dexamethasone.

Sp2 Expression Suppresses Root Growth

Growing roots are heavily engaged in cellular division and elongation, and they present a much simpler tissue structure than leaves for analysis of these events (Dolan and Roberts, 1995). In fact, NtSyr1 is most abundant in roots (Leyman et al., 2000), making this an appropriate tissue in which to examine the effects of Sp2 expression. Therefore, we measured root growth post-germination after placing seed on Murashige and Skoog (1962) (MS) medium with 0.7% Phytagel in Petri dishes placed vertically on end. Compared with the wild type and the 35S vector controls, *Sp1* transgenic plants showed a significantly enhanced rate of root growth during the first 14 days after germination (Figure 5A). *Sp2* transgenic plants showed a slight, but not significant, reduction in root growth during this period, and corresponding results were obtained with the *HSp1* and *HSp2* transgenic lines (data not shown).

We performed similar measurements with *dexSp2* and *dexC* (empty vector) transgenic plants, including 1 μM dexamethasone in the Phytagel medium. Dexamethasone at

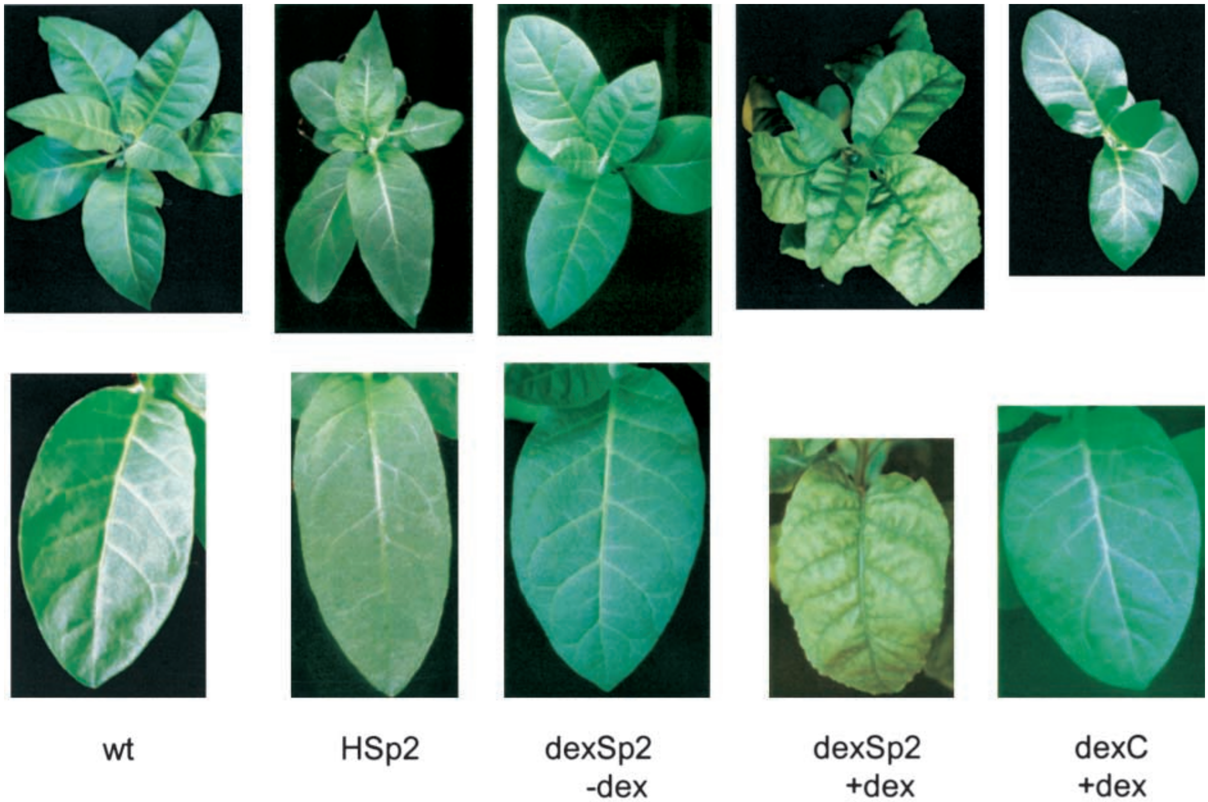

Figure 3. Sp2 Expression Alters Aerial Growth Characteristics and Leaf Morphology.

Full view (top row) and third expanded leaves (bottom row) from 7- to 8-week-old tobacco as labeled: wt (wild type), Hsp2 (*Hsp2-18*), dexSp2 (*dexSp2-14*), and dexC (*dexC2*). *dexSp2-14* and *dexC2* transgenic plants were treated with (+) and without (−) 10 μM dexamethasone (dex) at 24-hr intervals for 4 days before photographing.

concentrations as high as 30 μM had no adverse effects on initial germination, and similar results were obtained when plants germinated first on medium without dexamethasone and were transferred to dexamethasone-containing medium after germination (data not shown). Figure 5A includes measurements of root elongation after germination for *dexC2* and three *dexSp2* transgenic lines. Figure 5B summarizes the relative extent of growth inhibition on 1 μM dexamethasone for each of the transgenic lines together with protein gel blot analyses of Sp2 and RNA gel blot analyses of the GVG transcriptional regulator in each line taken from the germinated plants at the end of the experiment. Significant suppression of root growth was correlated with the level of Sp2, and not with the level of GVG expression (cf. lines *dexC1*, *dexSp2-11*, and *dexSp2-17*). Transgenic lines showing a low level of Sp2 expression also showed little reduction in the rate of root growth (Figure 5B, *dexSp2-3*, *dexSp2-4*, *dexSp2-12*, and *dexSp2-15*), and a moderate level of Sp2 expression also showed a partial suppression of root growth (Figures 5A and 5B, *dexSp2-10* and *dexSp2-16*), whereas lines with high levels of Sp2 expression showed virtually complete inhibition of growth once the roots reached a length of 3 to 5 mm (Figures 5A and 5B, *dexSp2-1* and *dexSp2-14*). Of the *dexC* transgenic lines carrying the empty vector, none showed any significant suppression of root growth on dexamethasone. Root growth in *dexSp2* transgenic plants in every case was fully reversible when plants were transferred to dexamethasone-free medium (data not shown). In the most strongly expressing lines, growth did not resume at the original root tip. Instead, these plants developed laterals, often close to the hypocotyl-root junction.

In agreement with these observations, longitudinal sections of root tips from *dexSp2* transgenic plants uncovered profound alterations in cell division and cellular morphology after treatments with dexamethasone. Figure 6 shows sections taken from seedlings of the *dexSp2-14* line and of the vector control line *dexC2* germinated on liquid MS medium and transferred at the start of the experiment to medium containing 1 μM dexamethasone. Again, transfer to the

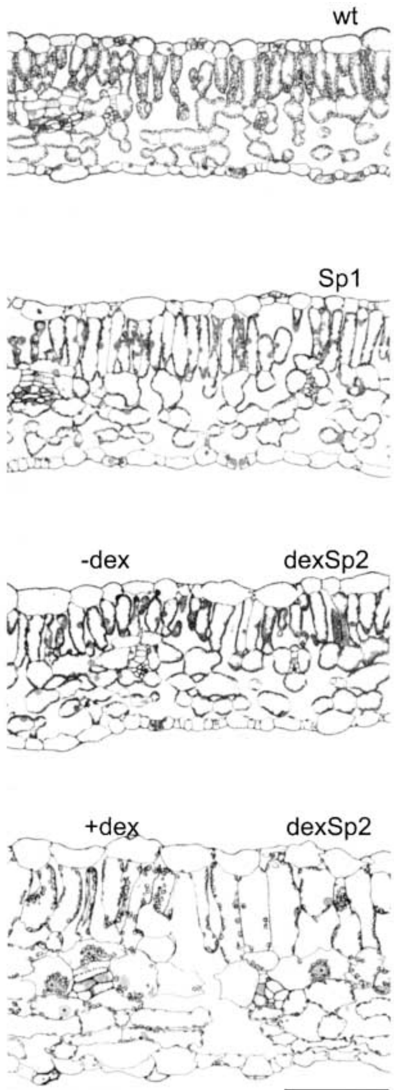

Figure 4. Sp2 Expression Alters the Cellular Morphology of the Leaf.

Cross-sections of third expanded leaves from 7- to 8-week-old tobacco: wt (wild type), Sp1 (*HSp1-4*), and dexSp2 (*dexSp2-14*) with (+) or without (−) 10 μM dexamethasone (dex) treatment (4 days at 24-hr intervals before harvesting). Sections were stained with toluidine blue. Vector controls (*dexC2* with or without dexamethasone and pCAMBIA1380; data not shown) were indistinguishable from the wild type and HSp1. Bar = 100 μm.

steroid led to a complete suppression of root growth in the *dexSp2* transgenic plants within 48 hr (data not shown). The most noticeable features associated with the dexSp2 transgenic plants in this case was a disruption of the radial symmetry, irregular expansion of cells at the tip, and an expansion and vacuolization of cells in the meristematic region of the tip. After 96 hr in dexamethasone, cells in the meristematic regions of these root tips contained a single large vacuole and commonly showed the nucleus to be positioned at the cell periphery rather than centrally. We counted the number of dividing cells within medial sections through tips of these plants and wild-type tobacco (Table 1). In the absence of dexamethasone, *dexSp2-14*, *dexC2* transgenic, and wild-type plants typically showed three or four dividing structures per section. Similar results were obtained for *dexC2* transgenic and wild-type plants exposed to dexamethasone. However, no dividing structures were found in root tips from *dexSp2-14* transgenic plants after 96 hr of exposure to 1 μM dexamethasone.

Sp2 Action on Growth Is Suppressed by Elevating NtSyr1 Expression

It is likely that Sp2 action in vivo is the consequence of its competition for protein partners that normally would interact with NtSyr1. This simple explanation accounts for the ability of Sp2 to interfere with abscisic acid–mediated control of guard cell ion channels (Leyman et al., 1999) and for the results of its expression on leaf and root morphology (see above). It also accords with the mechanics of SNARE function during vesicle fusion, which relies on intermolecular interactions between the cytosolic coiled-coil regions of the several SNARE proteins (Sutton et al., 1998; Jahn and Sudhof, 1999). These domains are cytosolic and therefore are potential targets for competition by soluble SNARE fragments. The Sp2 protein fragment lacks the C-terminal membrane anchor of NtSyr1 and would not be expected to substitute fully in the functioning of the intact syntaxin; instead, it might titrate out NtSyr1 partners and thereby reduce the formation of functional SNARE complexes (O'Connor et al., 1997). One prediction of this hypothesis is that the effects of Sp2 expression in planta should be suppressed when expression of the intact NtSyr1 protein is enhanced.

To test this idea directly, we crossed *Sp1* and *HSp1* transgenic plants with plants from the intermediately and strongly expressing *dexSp2* transgenic lines *dexSp2-10* and *dexSp2-14*, respectively (Figure 5). Plants carrying both transgenes were selected for growth on hygromycin and PPT. We found that the *Sp1*:*dexSp2* transgenic plants grown in the glasshouse were indistinguishable from wild-type plants. In contrast with the *dexSp2* parent lines (Figure 3), however, spraying with 20 μM dexamethasone had little effect on leaf development or aerial growth of progeny from either of the crosses, even after 10 days of repeated treatments (data not shown). To quantify the effects of enhanced NtSyr1 expression, we examined root growth of seedlings germinated in the presence and absence of 1 μM dexamethasone. Figure 7 shows that Sp1 overexpression was associated with nearly normal growth, as before (cf. Figure 5). However, unlike the *Sp2* transgenic plants, in the presence of dexamethasone root growth of the *Sp1*:*dexSp2*,

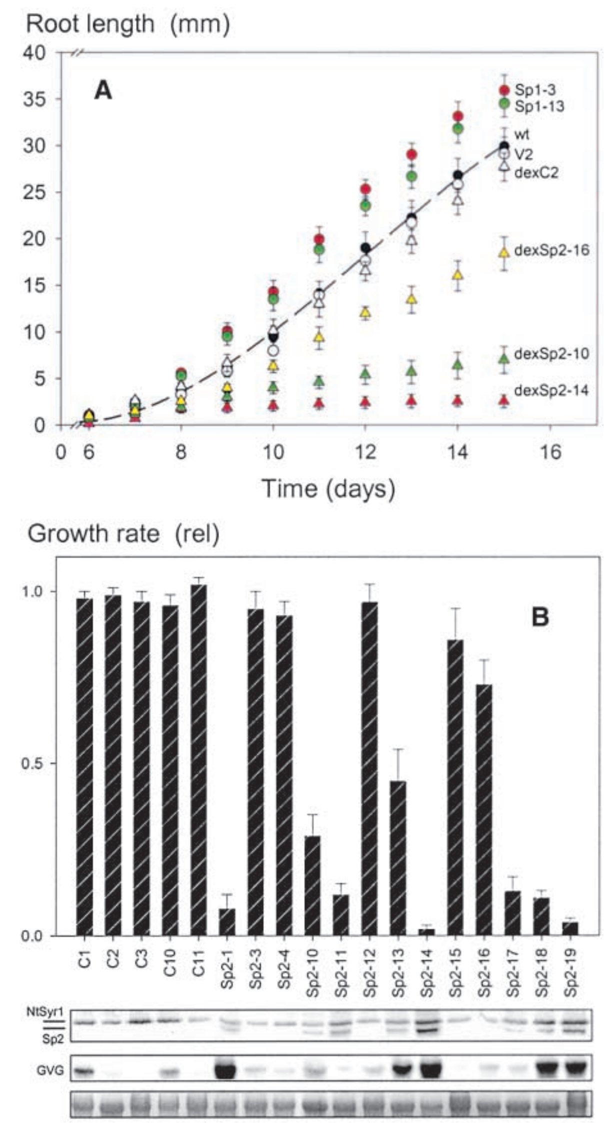

Figure 5. Root Growth of Seedlings Is Accelerated by Overexpression of NtSyr1 and Suppressed by the Sp2 Peptide.

Tobacco seed were germinated on solid MS medium, and root length was recorded at 24-hr intervals over 10 days after germination (see Methods).

(A) Time course of growth for wild-type (wt) tobacco and representative transgenic lines. Sp1-3, Sp1-13, and V2 (empty 355-vector) lines were grown on standard MS medium. *dexC2* (vector), *dexSp2-16* (weak expressor), *dexSp2-10* (moderate expressor), and *dexSp2-14* (strong expressor) were grown in the presence of 1 μM dexamethasone. Growth of all *dexSp2* lines was indistinguishable from that of the vector control in the absence of dexamethasone (data not shown). Data are means ±SE of four independent experiments, each with 20 seed.

(B) Correlation of root growth with Sp2 expression under dexamethasone control. Top, growth expressed as the relative (rel) growth rate with or without 1 μM dexamethasone 10 to 12 days after germination. Bottom, analysis of protein and total RNA (10 μg/lane) extracts from seedlings of each line. Protein gel blot analysis of Sp2 expression using anti-Sp2 antibody as a probe (top row) and RNA gel blot analysis of dexamethasone transactivator expression using radiolabeled GVG DNA as a probe (middle row) are shown. rRNA was visualized by ethidium bromide staining as a control for loading (bottom row). Positions of NtSyr1 and Sp2 peptide bands are indicated.

seedlings continued at nearly normal rates. Protein gel blot analysis of the seedlings (Figure 7B) confirmed that this rescue of growth was associated with constitutively high levels of NtSyr1: overexpression of NtSyr1 corresponded to that of the *Sp1* transgenic plants, but in this case it was seen together with the background of dexamethasone-inducible expression of Sp2 similar to that in each of the parent *dexSp2* transgenic lines. Even 8 to 10 days after germination on dexamethasone, these seedlings were indistinguishable from the wild-type and *Sp1* transgenic seedlings (Figure 7A).

In addition, we performed root growth measurements of the *dexSp2-10*, *dexSp2-14*, and *dexC2* transgenic lines under salt stress, conditions that normally enhance NtSyr1 expression in tobacco (Leyman et al., 2000). Because high-osmotic-strength solutions inhibit germination, root growth was examined from seedlings grown for 7 days on standard MS medium and transferred subsequently to medium containing either 1 μM dexamethasone alone or in combination with NaCl (100 mM) or sorbitol (200 mM). Salt stress, like treatment with abscisic acid, induces NtSyr1 expression transiently over a period of ∼24 hr. Therefore, roots were measured 3 days after transfer, and new growth was calculated from the time of transfer from standard MS medium. As expected, expression of Sp2 induced by 1 μM dexamethasone suppressed root growth in the *dexSp2-10* and *dexSp2-14* transgenic lines. However, the effect of Sp2 expression was relaxed partially in *dexSp2-14* transgenic plants and to a greater extent in *dexSp2-10* transgenic plants after transfer to medium containing 100 mM NaCl or 200 mM sorbitol (Figure 8). Thus, genetic and environmental manipulation of NtSyr1 expression is sufficient to counter the effects of Sp2 expression on tobacco growth and morphology.

Expression of Sp2 Blocks Transport of a Secreted Yellow Fluorescent Protein/GFP Marker to the Apoplast

Expansive cell growth is tied closely to vesicular traffic and secretion (Blatt et al., 1999) and the effects of Sp2, and their titration against NtSyr1 expression thus also supports an immediate role for the syntaxin in secretory transport. To examine directly the action of Sp2 on membrane traffic to the

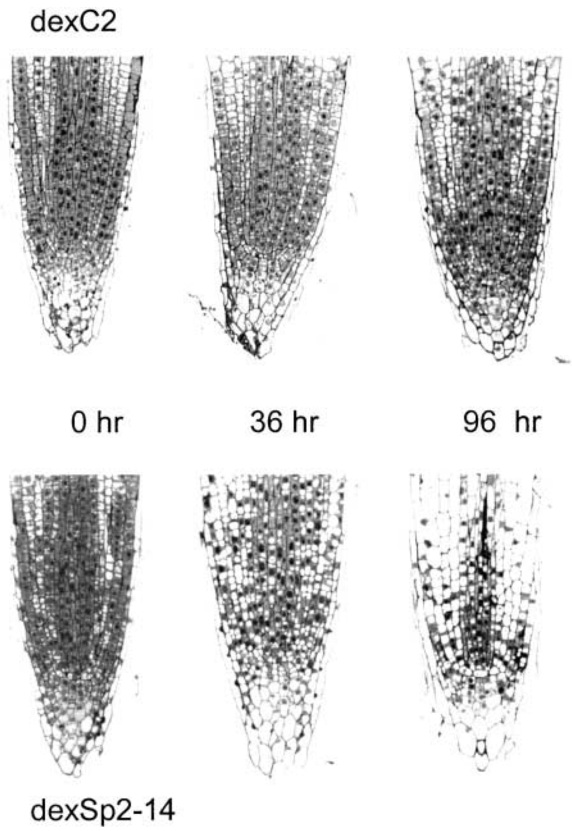

Figure 6. Sp2 Expression Disrupts the Apical Organization of the Root Tip.

Longitudinal sections through root tips of tobacco *dexC2* and *dexSp2-14* transgenic lines in the absence of dexamethasone and at 36 and 96 hr after transfer to MS medium containing 1 μM dexamethasone.

apoplast, we used an assay based on intracellular accumulation of a GFP variant, secGFP, that normally is secreted to the apoplast (Batoko et al., 2000). When secreted, secGFP fails to build up in a fluorescent form, but it accumulates and is visualized readily in the endomembrane organelles when transport to the apoplast is inhibited. *A. tumefaciens*–mediated transfection by infiltration was used to transiently coexpress secGFP with Sp1 or Sp2 in leaves of tobacco, and secGFP accumulation was monitored by confocal laser scanning microscopy of the lower epidermal cells. Sp1 and Sp2 expression was confirmed by protein gel blot analysis of the transfected leaves (data not shown).

Figure 9 shows results from one set of experiments, with similar results obtained in each of four additional sets of experiments. Expression of secGFP alone (data not shown) or together with the full-length NtSyr1 protein (Figure 9A) resulted in no intracellular accumulation and a weak apoplastic fluorescence that was detected only at high magnification when the laser excitation was attenuated weakly or not at all. Coexpression of secGFP with Sp2, however, led to a large increase in secGFP fluorescence that was visible clearly within the epidermal cells (Figure 9B).

We also examined the effects on secGFP transport of dexamethasone-mediated Sp2 expression. In this case, *A. tumefaciens* carrying the secGFP expression plasmid was infiltrated with or without 10 μM dexamethasone in leaves of *dexSp2-14* and, as a control, *dexC2* transgenic tobacco. In separate experiments, dexamethasone was applied by spraying as described above, with similar results (data not shown). As expected, no accumulation of secGFP fluorescence was observed after transfection without dexamethasone in leaves of *dexSp2-14* transgenic plants (Figure 9C) or in *dexC2* transgenic tobacco, either with or without the inclusion of dexamethasone (data not shown). At high magnification, cytosolic streaming was observed and the cells excluded propidium iodide fluorescence used as an extracellular marker (Figure 9C, inset), confirming viability. With dexamethasone, secGFP accumulation was visible in *dexSp2-14* transgenic plants (Figures 9D and 9E). Significantly, the effects of Sp2 expression on secGFP accumulation were evident within 24 to 48 hr, well before any visible phenotype associated with Sp2 induction. Cells that accumulated secGFP also excluded propidium iodide over 5 to 7 days (Figure 9D, inset) while maintaining apparently normal cytoplasmic streaming, endoplasmic reticulum (ER), and Golgi dynamics. Furthermore, no secGFP fluorescence was observed in the presence of dexamethasone in parallel experiments with *Sp1*:*dexSp2-14* transgenic plants (data not shown). These observations make it unlikely that blocking of secGFP secretion was the consequence of a loss in cell viability or of nonspecific effects of Sp2 expression. Instead, they support the conclusion that dexamethasone-mediated expression of Sp2 was sufficient to disrupt membrane traffic to the plasma membrane and secretion to the apoplast.

At higher resolution, secGFP was seen to accumulate principally within the nuclear envelope and a dynamic reticulate organelle typical of the ER (Figure 9D). In many cells, secGFP also was observed in punctate structures that

Table 1. Dexamethasone-Induced Expression of the Sp2 Fragment Halts Cell Division at the Root Tip

	Without Dexamethasone	With Dexamethasone
Wild type	3.6 ± 0.6 (5)	3.3 ± 0.7 (4)
dexC2	3.2 ± 0.2 (4)	3.4 ± 0.9 (3)
dexSp2-14	3.0 ± 0.7 (4)	0.0 ± 0.0 (5)

Dividing initial cells expressed as means ±SE of cells observed late in division (anaphase and telophase) per section for (*n*) root tips after 96 hr with or without 1 μM dexamethasone.

moved over the ER network. These structures usually were dim relative to the network and, because of their high mobility, often were indistinct in static images (see below). Given the proposed role of NtSyr1 at the plasma membrane (Leyman et al., 1999, 2000), the accumulation of secGFP principally in the ER and nuclear envelope rather than in the Golgi or post-Golgi structures was not expected. One possible explanation was that Sp2 action caused secGFP to accumulate in the Golgi apparatus as well as in the ER and that the mobile punctate structures represented the Golgi stacks (Boevink et al., 1998). Alternatively, Sp2 expression might have disrupted the Golgi, resulting in secGFP accumulation in the upstream ER compartment.

To monitor Sp2-mediated secretory block while visualizing the Golgi, we developed a new glycosylated secretory marker, *N*-secYFPΔC, by exchanging the GFP coding sequence of secGFP (Batoko et al., 2000) for that of yellow fluorescent protein (YFP). We used the GFP-based Golgi marker *N*-ST-GFP (Boevink et al., 1998; Batoko et al., 2000) to monitor the structure and position of the Golgi stacks. The YFP spectral variant of GFP thus enabled double labeling of the Golgi stacks (using *N*-ST-GFP) and of secretory block by Sp2 (using *N*-secYFPΔC) after selecting appropriate imaging parameters to discriminate GFP and YFP fluorescence. Figures 10A to 10F show that, expressed on its own, *N*-secYFPΔC, like secGFP, accumulated poorly and was difficult to visualize (Figures 10A and 10D), but when coexpressed with the dominant negative mutant AtRab1b(N121I) that inhibits ER-to-Golgi transport (Batoko et al., 2000), it accumulated strongly within the ER network (Figures 10C and 10F). Coexpression with Sp2 also resulted in the accumulation of YFP fluorescence (Figures 10B and 10E), although the effect was weaker than with AtRab1b(N121I). When *N*-secYFPΔC was coexpressed with *N*-ST-GFP in double-labeling experiments, the GFP-labeled Golgi stacks appeared similar in size, number, and mobility in both the absence and presence of Sp2 expression, even in cells that showed strong accumulation of *N*-secYFPΔC (cf. Figures 10G and 10H with 10I and 10J). We also were unable to identify any effect of Sp2 in the redistribution of *N*-ST-GFP from the Golgi to the ER, in contrast to AtRab1b (Batoko et al., 2000). These observations show that Sp2-induced accumulation of *N*-secYFPΔC and secGFP in the ER cannot be explained by a loss or gross disorganization of the Golgi apparatus.

Although Sp2 expression led to *N*-secYFPΔC accumulation primarily in the ER, as with secGFP, mobile punctate structures often were visible in high resolution images (Figure 10E, arrows). Strikingly, in some cells, we observed *N*-secYFPΔC to accumulate primarily in these structures, where it colocalized with *N*-ST-GFP in both images (Figures 10K to 10M) and transect profiles (Figure 10N), indicating that the punctate structures probably represent Golgi stacks. Such cells were not observed when secGFP or *N*-secYFPΔC were coexpressed with the dominant inhibitory At-Rab1b(N121I). The image shown in Figures 10K to

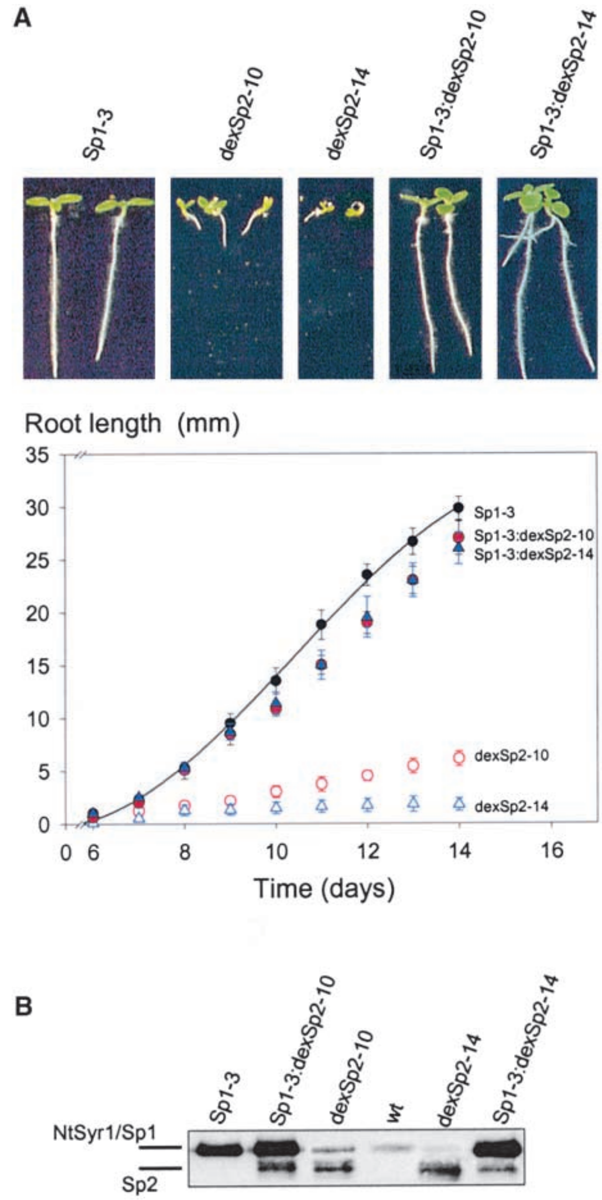

Figure 7. Enhancing the Expression of NtSyr1 Suppresses the Effects of the Sp2 Peptide on Root Growth.

(A) Seed of wild type and crosses between transgenic tobacco lines were germinated on solid MS medium with 1 μM dexamethasone, and root length was recorded at 24-hr intervals over 10 days after germination (see Figure 5). Top, images from day 14 after sowing; bottom, time course of root growth as a function of days after sowing. Data are means of 20 seedlings in each case. Crosses were of the 35S-driven NtSyr1 transgenic line *Sp1-3* (similar results with *HSp1-10* are not shown) to the moderately expressing *dexSp2-10* and the strongly expressing *dexSp2-14* dexamethasone-inducible lines.

(B) Analysis of protein (12 μg/lane) extracts from seedlings of each line. Protein gel blot analysis of Sp2 expression using anti-Sp2 antibody as a probe. NtSyr1 (Sp1) and Sp2 peptide bands are indicated. wt, wild type.

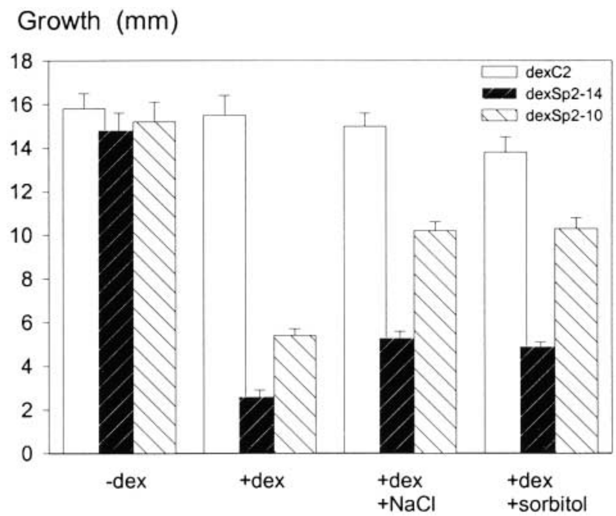

Figure 8. Enhancing the Expression of NtSyr1 under High Salt and Osmotic Stress Suppresses the Effects of the Sp2 Peptide on Root Growth.

Growth is expressed as the increment 3 days after transfer to MS medium alone (−dex) or with additions of 1 μM dexamethasone, 100 mM NaCl, and 200 mM sorbitol. Data in each case are means ±SE for 10 plants each of the *dexC2* (vector control), *dexSp2-10*, and *dexSp2-14* transgenic lines.

10M includes one cell in which *N*-secYFPΔC labeled punctate structures (Figures 10K and 10M, arrows) in association with a relatively dim ER network and a second cell in which *N*-secYFPΔC accumulation is visible only in punctate structures (Figures 10K and 10M, arrowheads). Although the YFP signal in these cells is relatively weak, when control samples coexpressing *N*-ST-GFP and *N*-secYFPΔC (Figures 10O to 10Q) or an ER-targeted GFP alone (Figures 10R to 10T) were imaged under identical conditions, there was virtually no GFP signal in the YFP image (Figures 10O to 10T), excluding the possibility that these punctate structures resulted from bleed-through from GFP to the YFP channel of the microscope. The profiles of the GFP and YFP signals along the transects (see images) show quantitatively the extent of bleed-through under these conditions (Figures 10N, 10Q, and 10T), confirming a peak in the YFP signal corresponding to the position of the Golgi in cells expressing Sp2 (Figure 10N).

In contrast, when coexpressed with the mutant AtRab1b(N121I), both *N*-ST-GFP and *N*-secYFPΔC accumulated in the ER, but *N*-secYFPΔC label was not found in the Golgi (Figures 10U to 10W). When the profiles of the *N*-ST-GFP and *N*-secYFPΔC signals were analyzed along a stand of ER, we did not find peaks in the YFP signal coinciding with the positions of the *N*-ST-GFP–labeled Golgi stacks, although the GFP and YFP profiles were very similar elsewhere along the stand (Figure 10W). These observations are consistent with the previous conclusion that AtRab1b(N121I) does not cause accumulation of secGFP in the Golgi apparatus (Batoko et al., 2000), and they show that Sp2 and AtRab1b(N121I) exert distinct effects on trafficking of secGFP and *N*-secYFPΔC to the apoplast.

DISCUSSION

It is the cytosolic domains of each of the several SNARE proteins that interact to form a stable complex when a vesicle docks at its target site (Jahn and Sudhof, 1999). In neurons, these interactions are a prelude to vesicle fusion and are essential for exocytosis and neurotransmitter release (Hanson et al., 1997; Wu et al., 1999). Eliminating the coiled-coil domains of SNAP-25 or syntaxin 1A (e.g., by cleavage with *Botulinum* toxins) prevents fusion, and a similar block of exocytosis results in the introduction of peptides corresponding to key interacting domains of these SNARE proteins (Hayashi et al., 1995; O'Connor et al., 1997; Ferrer Montiel et al., 1998; O'Sullivan et al., 1999; Scales et al., 2000). In the latter case, the peptides compete effectively for protein partners and titrate away these elements essential for fusion. Furthermore, the effects of disrupting SNARE partner interactions can extend to other events of neurotransmitter release and vesicle recycling, including the regulation of ion channels at the plasma membrane (Degtiar et al., 2000).

It is almost certain that similar interactions between SNARE proteins and related secretory elements contribute to vesicle trafficking and fusion in plants. Representatives of each of the protein partners are known to occur in vegetative tissues (Blatt et al., 1999; Sanderfoot and Raikhel, 1999), secretion through the endomembrane system is sensitive to common secretory antagonists such as brefeldin A (Kunze et al., 1995; Satiat Jeunemaitre et al., 1996; Boevink et al., 1998; Steinmann et al., 1999), and a 20S protein complex of SNARE proteins was demonstrated recently in Arabidopsis (Bassham and Raikhel, 1999). Previously, we identified a syntaxin from tobacco, NtSyr1, that is associated with cellular signal transduction in response to abscisic acid, drought, and salt stress and that is expressed throughout the plant (Leyman et al., 1999, 2000). When injected in guard cells, the cytosolic domain of NtSyr1, the so-called Sp2 peptide, interfered with the regulation of K^+ and Cl^- channels by abscisic acid (Leyman et al., 1999). The data presented above now demonstrate that expression of this same peptide domain affects the cellular growth and development of aerial and root tissues and that it interferes with secretion in stably transformed tobacco in a manner that is specific to the NtSyr1 protein. These results support a role for NtSyr1 in vesicle traffic at the plasma membrane and are consistent with a general requirement for the protein in cellular growth and homeostasis.

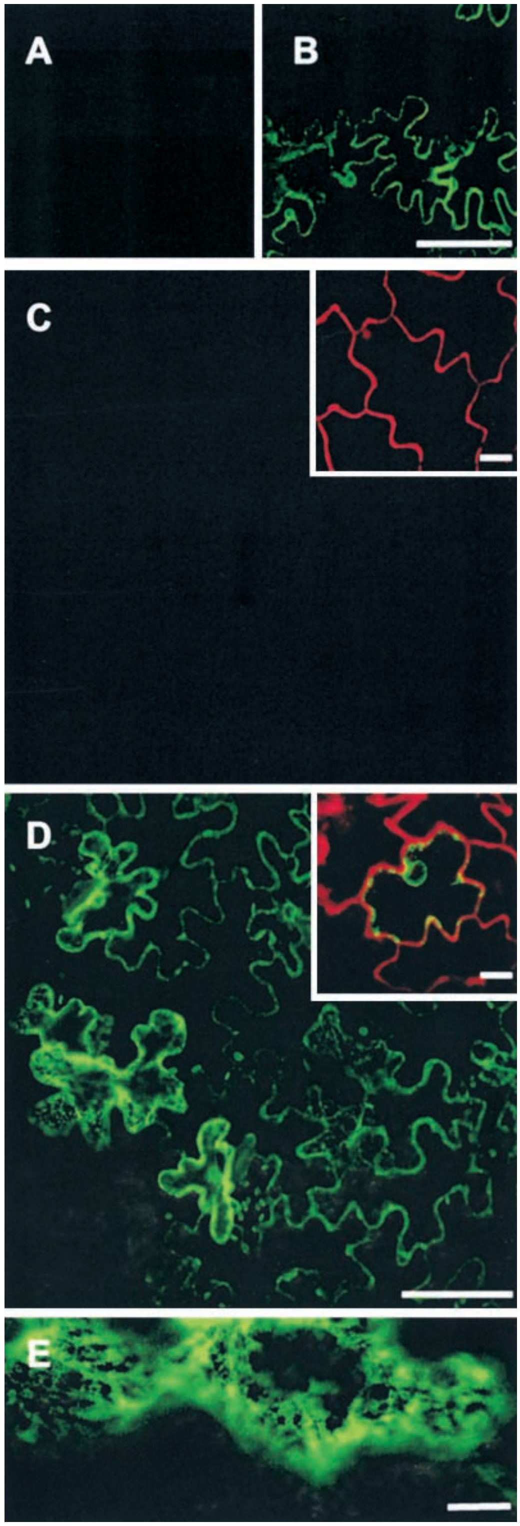

Figure 9. Expression of Sp2 Blocks Secretion and Leads to the Accumulation of secGFP within a Cytosolic Reticulum.

Confocal images at low magnification of wild-type tobacco leaf epidermis transfected to express secGFP together with Sp1 **(A)** and with Sp2 **(B)** and of *dexSp2-14* transgenic tobacco leaf epidermis transfected to express secGFP in the absence **(C)** and presence (**[D]** and **[E]**) of 1 μM dexamethasone. **(E)** shows a high magnification confocal image of a *dexSp2-14* transgenic tobacco leaf epidermis transfected with secGFP in the presence of 1 μM dexamethasone. Insets show the same tissue after infiltration with propidium iodide as a marker for extracellular space and testing for cell viability by dye exclusion.

Bars in **(A)** to **(D)** = 100 μm; bar in **(E)** = 10 μm.

Sp2 Action Is Specific to NtSyr1 Function

Three major lines of evidence point to a toxicity of the Sp2 peptide and indicate that it interferes specifically with the normal functioning of NtSyr1. The first, albeit indirect, hint of such toxicity comes from the success of recovery for each of the transformations. Large numbers of independent *NtSyr1*- (*Sp1*-) and *HSp1*-transformed lines were obtained with constructs driven by the 35S promoter, and without exception, these lines gave reproducibly high levels of NtSyr1 protein, estimated to be ~20-fold the normal levels of the endogenous protein. In contrast, a relatively small number of lines were recovered from transformations with the *HSp2* construct driven by the 35S promoter in the same cassette, and of these, fewer than one-quarter showed any measurable expression of the Sp2 peptide. Much higher levels of Sp2 expression could be obtained, but only when transformations were performed with the *dexSp2* construct and Sp2 expression was induced in the presence of dexamethasone. Thus, despite the strong 35S promoter used in each case for NtSyr1, HSp1, and HSp2 expression, there appeared a counter-selection against plants carrying the *HSp2* gene.

Consistent with these observations, the second line of evidence lies in the phenotypes recovered in each case. Plants overexpressing the full-length NtSyr1 and HSp1 proteins were largely indistinguishable from the wild type and vector controls, apart from an increase in the rates of root growth of seedlings. In contrast, even moderate expression of the Sp2 peptide was associated with a disturbance of aerial tissue morphology. High levels of Sp2 expression were accompanied by a complete cessation of aerial and root growth and a loss of meristematic structure in the root tip. At first glance, the relatively mild effects on growth of NtSyr1 and HSp1 is surprising, given the ~20-fold increase in expression over that of the wild type (Figure 1). However, when overexpressed, much of the additional protein is associated with intracellular membranes rather than the plasma membrane, where it might otherwise have a physiological impact (Leyman et al., 2000).

Finally, we demonstrated that increasing the levels of NtSyr1 in the plant alleviated the effects of Sp2 expression on growth and tissue morphology. Dexamethasone-induced

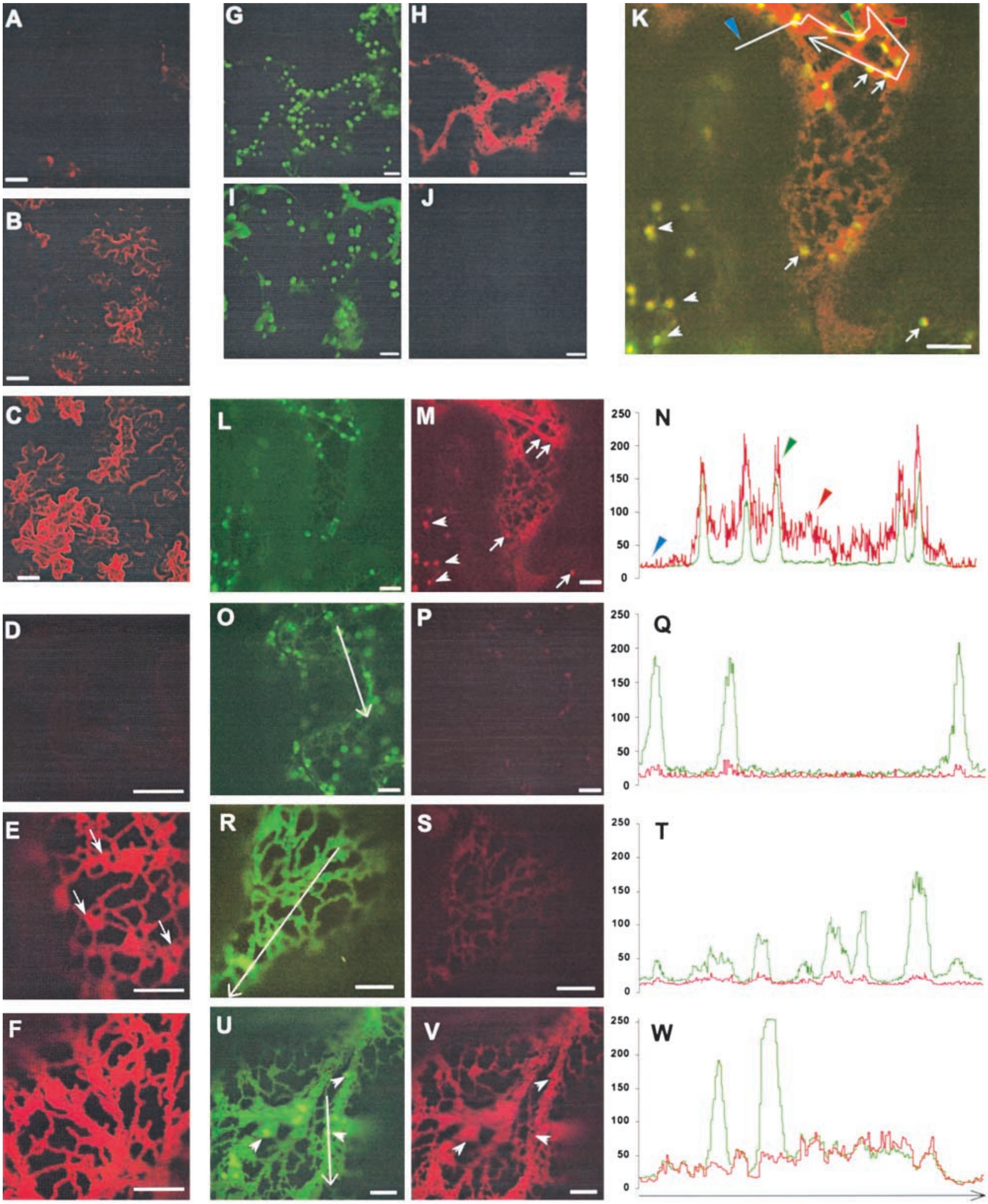

Figure 10. Sp2-Mediated Accumulation of Secreted *N*-secYFPΔC Differs from That Observed with the Dominant Negative Mutant AtRab1b(N121I) and Colocalizes with Golgi-Targeted *N*-ST-GFP.

expression of the Sp2 peptide had no effect on plants that also constitutively expressed high levels of the full-length NtSyr1 protein under the control of the 35S promoter (Figure 7), and the effect of Sp2 in suppressing root growth was reduced when NtSyr1 expression was enhanced in wild-type tobacco by salt and osmotic stress (Figure 8). Furthermore, we found no evidence of an increase in initial or multinucleate cells within the root meristem that might indicate cells "trapped" late in division. Such trapping is characteristic of the *knolle* syntaxin mutant of Arabidopsis, which shows some similarity with NtSyr1 and its Arabidopsis homolog AtSyr1 (Leyman et al., 1999). Indeed, to the contrary, we found no dividing initial cells in the roots of Sp2-expressing plants.

The latter observations are especially significant, because they imply that Sp2 action is targeted specifically to NtSyr1 in vivo. At least in vitro, the interactions between mammalian SNARE proteins often are promiscuous (Pfeffer, 1996; Avery et al., 1999; Fasshauer et al., 1999; Yang et al., 1999), an observation that has increased speculation that these interactions might not contribute to the specificity of vesicle trafficking (Hanson et al., 1997; Nichols and Pelham, 1998; Jahn and Sudhof, 1999). In yeast, genetic deletion of several SNARE proteins has been possible without significant physiological consequences, and in other cases, overexpression of distantly related SNARE proteins was found to be sufficient to rescue the loss of some trafficking functions (Aalto et al., 1993; Holthuis et al., 1998; Nichols and Pelham, 1998; von Mollard and Stevens, 1999). By the same arguments, we could imagine that the Sp2 peptide might interfere with SNARE interactions other than those associated with NtSyr1 and thus generate a set of phenotypes unrelated to the normal functioning of the wild-type protein. This interpretation is not reconciled easily with our data. The fact that normal growth was rescued, even in the presence of the Sp2 peptide, indicates an action specific to NtSyr1 that was overcome simply by increasing the "dosage" of wild-type protein. In fact, Scales et al. (2000) came to a very similar conclusion. Their experiments have shown that block and rescue of norepinephrine secretion in vivo is specific to a subset of plasma membrane SNARE proteins. A recent in vitro analysis of SNARE interactions contributing to yeast endomembrane trafficking supports this interpretation (Fukuda et al., 2000; Mcnew et al., 2000; Parlati et al., 2000).

Rescue of the Sp2 phenotype by overexpressing NtSyr1 also discounts the argument that the effects of the peptide were associated with the dexamethasone GVG activator and not with the syntaxin per se. Recently, Kang et al. (1999) reported growth defects in Arabidopsis transformed with the empty pTA7002 dexamethasone expression vector used in this study. The growth impairment was correlated with RNA levels of the GVG transcription factor used to drive dexamethasone-stimulated expression. Analysis of our transgenic lines did not reveal a strong correlation with the GVG transcript (Figure 5). The fact that growth could be rescued, even in lines that strongly expressed the transcription factor, supports this conclusion.

NtSyr1 Is Essential for Traffic to the Plasma Membrane

Our data now provide concrete evidence of a role for NtSyr1 in vesicle trafficking. Previous experiments had failed to

Figure 10. (continued).

(A) to **(F)** Confocal images at low (**[A]** to **[C]**) and high (**[D]** to **[F]**) magnification of tobacco leaf epidermis transfected to express *N*-secYFPΔC only (**[A]** and **[D]**), *N*-secYFPΔC with Sp2 (**[B]** and **[E]**), and *N*-secYFPΔC with AtRab1b(N121I) (**[C]** and **[F]**). Arrows in **(E)** identify mobile punctate structures observed in the presence of Sp2. Bars in **(A)** to **(C)** = 50 μm; bars in **(D)** to **(F)** = 5 μm.

(G) to **(J)** Cotransfection for expression of *N*-secYFPΔC and *N*-ST-GFP shows similar characteristics of Golgi labeling with (optical section image pairs in **[G]** and **[H]**) and without (optical section image pairs in **[I]** and **[J]**) Sp2. GFP (**[G]** and **[I]**) fluorescence uncovers punctate structures in either case; YFP fluorescence is evident when coexpressed with Sp2 **(H)** but not in its absence **(J)**. Note the cell central to the image pair in **(G)** and **(H)** shows particularly strong accumulation of *N*-secYFPΔC without any apparent alteration in *N*-ST-GFP Golgi labeling. Compare this with the cell (top right) that shows little or no *N*-secYFPΔC accumulation. Bars = 5 μm.

(K) to **(W)** Cotransfection for expression of *N*-secYFPΔC and *N*-ST-GFP with Sp2 (optical section image pairs in **[L]** and **[M]**; merged image in **[K]**; transect pixel intensities [see **(K)**] in **[N]**) demonstrates colocalization of fluorescence signals in cells with moderate to weak *N*-secYFPΔC accumulation. In one cell (lower left), *N*-secYFPΔC accumulation is visible only in the punctate structures (**[K]** and **[M]**, arrowheads). Similar structures are visible in the second cell (**[K]** and **[M]**, arrows) against the weak background of *N*-secYFPΔC fluorescence in the reticulate network. Compare the locations with that of *N*-ST-GFP labeling of the Golgi **(L)**. **(N)** shows pixel intensities (from the transect shown in **[K]**) for GFP (green trace) and YFP (red trace) showing coalignment of intensity peaks. Image pairs on expression of *N*-secYFPΔC and *N*-ST-GFP without Sp2 (optical section image pairs in **[O]** and **[P]**; transect pixel intensities [see **(O)**] in **[Q]**) obtained under identical conditions (see Methods) show the absence of *N*-secYFPΔC accumulation. *N*-ST-GFP fluorescence (**[O]**, green trace in **[Q]**) and *N*-secYFPΔC signal (**[P]**, red trace in **[Q]**). Image pairs (**[R]** and **[S]**; transect pixel intensities [see **(R)**] in **[T]**) on expression of ER-targeted GFP-HDEL are controls to show the extent of fluorescence bleed-through from GFP (**[R]**, green trace in **[T]**) into the YFP acquisition channel (**[S]**, red trace in **[T]**). Image pairs (**[U]** and **[V]**; transect pixel intensities [see **(U)**] in **[W]**) on expression of *N*-secYFPΔC and *N*-ST-GFP with AtRab1b(N121I) shows the accumulation of both fluorescent labels in the reticulum but of *N*-ST-GFP only in the punctate structures. *N*-ST-GFP (**[U]**, green trace in **[W]**) and *N*-secYFPΔC (**[V]**, red trace in **[W]**) fluorescence images. Note the coincidence of pixel intensities **(W)** across the transect, except where it crosses over the two punctate structures. Bars in **(L)** to **(V)** = 5 μm.

demonstrate NtSyr1-mediated rescue of growth in mutant yeast carrying a double deletion of the Sso1/Sso2 plasma membrane syntaxins (Leyman et al., 1999). These results left open the question of functional conservation between the yeast and plant syntaxins. Using the apoplastic marker secGFP (Boevink et al., 1999) and a new variant *N*-secYFPΔC, we now show that expression of the Sp2 peptide, but not of the full-length syntaxin, interfered with secretion, leading to an accumulation of these markers within the endomembrane system (Figures 9 and 10). Similar results were obtained in *dexSp2* transgenic plants transiently expressing secGFP in the presence of dexamethasone, and overexpression of Sp1 also suppressed the accumulation of GFP in plants expressing Sp2, indicating that the effect is specific to NtSyr1-mediated secretion.

We found that *N*-secYFPΔC and secGFP each accumulated in the ER and Golgi when coexpressed with Sp2. NtSyr1 normally is localized to the plasma membrane (Leyman et al., 2000), and the Sp2 fragment has been shown to affect the activities of several ion channels at this membrane (Leyman et al., 1999). So a role for NtSyr1 in vesicle traffic at the plasma membrane might be anticipated. This conclusion would be consistent with the observed accumulation of *N*-secYFPΔC in the Golgi and ER if Sp2 action led secondarily to an accumulation of secreted markers in upstream compartments. However, our data do not distinguish between several possible mechanisms that could underlie such action. For example, the inhibition of fusion at the plasma membrane might suppress vesicle formation at the Golgi. It also is plausible that Sp2 might contribute to intra-Golgi transport in addition to functioning in post-Golgi transport. Nor can we exclude the possibility that NtSyr1 and Sp2 influence a recycling pathway from the plasma membrane to the Golgi and that the inhibition of forward traffic we observed was a secondary consequence of the failure to recycle a membrane component essential for its maintenance. These same explanations apply equally to Sp2-induced accumulation of the secreted markers in the ER. Until now, studies of traffic to the plasma membrane using secGFP and related markers have dealt almost exclusively with trafficking events between the Golgi and the ER (Batoko et al., 2000; Takeuchi et al., 2000; but also see Jin et al., 2001). It remains to be established whether, in general, these markers accumulate only in the organelle immediately upstream of a given trafficking step when this step is blocked or whether organelles farther upstream also accumulate label.

We suspect that the Sp2 fragment affects some aspect of post-Golgi transport. The pattern of labeling in the presence of Sp2 contrasted with the effects of the inhibitory (dominant negative) mutant AtRab1b(N121I) that leads to accumulation of these fluorescent markers exclusively in the ER (Figures 10U to 10W) (Batoko et al., 2000). It also differs from the ER localization of secGFP observed in the presence of brefeldin A (Boevink et al., 1999). Sp2 failed to induce an accumulation of *N*-ST-GFP in the ER, in contrast to the mutant AtRab1b(N121I). Furthermore, we found cells that accumulated *N*-secYFPΔC poorly and primarily in the Golgi in the presence of Sp2 (Figures 10K and 10N). We interpret the latter to be cells showing the weakest Sp2 phenotype, probably the result of low Sp2 expression, and therefore to reflect the primary stages of marker accumulation in contrast to cells that showed higher levels of accumulation, and then in both the Golgi and the ER (see above).

These arguments aside, we cannot wholly exclude a nonspecific, if partial, inhibition of secGFP transport from the ER to the Golgi apparatus. At least in vitro SNARE interactions can be highly promiscuous (Avery et al., 1999; Fasshauer et al., 1999), although the same is probably not true in vivo (Mcnew et al., 2000; Scales et al., 2000; and above). Furthermore, this interpretation is not reconciled easily with the rescue of secretion by the overexpression of NtSyr1 in *Sp1:dexSp2-14* transgenic plants. Nonetheless, if NtSyr1 were to interact directly with Sp2 in vivo, it might titrate its activity directly and independent of Sp2 specificity. Resolving these issues will depend on the analysis of simple loss-of-function mutants and on the development of transport assays with greater temporal resolution.

Is Sp2 Action on Growth and Development a Consequence of Secretory Block?

At present, there is little functional detail that can be brought to bear on SNARE proteins in plants, although there is good reason to expect a high degree of specialization in their roles within the cell (Conceicao et al., 1997; Sato et al., 1997; Sanderfoot et al., 2001) (see Introduction). Only for the Arabidopsis *knolle* mutant has a specific activity in vivo been linked unambiguously to a SNARE protein. The *KNOLLE* gene encodes a syntaxin homolog that contributes exclusively to the formation of the cell plate during division (Lukowitz et al., 1996; Lauber et al., 1997). Mutant embryos show abnormal radial growth, and because cell wall deposition is incomplete, daughter cells fail to separate, become multinucleate, and are “locked” in the formation of the cell plate (Lauber et al., 1997).

SNARE proteins aside, interfering with secretory processing can have profound effects on cellular development and tissue organization. The *vcl1* mutant of Arabidopsis, an ortholog of the yeast Vps16p, fails to develop vacuoles and leads to embryo lethality (Rojo et al., 2001). A second Arabidopsis mutant, *gnom* (*emb30*), disrupts apical–basal polarity and loss of some organ structures (Mayer and Marshall, 1993; Shevell et al., 1994). The *GNOM* gene encodes an ADP-ribosylation factor (ARF) GTPase nucleotide exchange factor, and its mutation leads to a loss of the polar distribution of the Pin-1 protein, a putative auxin efflux carrier at the plasma membrane, similar to the effect of treatments with the ARF GTPase antagonist brefeldin A (Steinmann et al., 1999). Brefeldin A itself inhibits root growth and promotes radial expansion at low doses, consistent with its action on secretion (Baskin and Bivens, 1995).

Given the importance of secretory trafficking to the plasma membrane, it is not surprising that its disruption should have effects on cellular and tissue morphology. The plant cell must incorporate new cell wall material and membrane to accommodate the increase in cell surface area that accompanies an increase in cell volume. Indeed, even without growth, the flux of membrane material and protein through vesicle trafficking is essential for cellular homeostasis (Thiel and Battey, 1998). Disturbing membrane traffic to (and from) the plasma membrane might be expected to alter cell form through effects on the cell wall, ion transport, and osmotic balance (Morris and Robinson, 1998; Thiel and Battey, 1998; Battey et al., 1999) and to influence patterns of cell expansion and maturation (Blatt et al., 1999). So the effects of expressing the Sp2 peptide on aerial and root morphology and growth are broadly consistent with its action on secretion.

Indeed, we found that tobacco expressing the Sp2 peptide showed alterations in leaf form and a slowing of root growth in seedlings. With high levels of Sp2 expression, growth ceased altogether and the leaves developed an irregular and mottled surface associated with hypertrophy and disturbed patterns of cellular expansion within the lamina (Figures 3 and 4). Although we cannot say at present whether Sp2 expression also affected cell division in the leaves, in the roots it is clear that patterns of both cell division and expansion were perturbed. Normally, anticlinal cell division in the root tip gives rise to meristematic cells that contribute to files of differentiating cells behind the root tip (Dolan and Okada, 1999; Scheres and Heidstra, 1999). In plants expressing the Sp2 peptide, however, cell division appeared to cease, the organization of the cell files was disturbed, and cells of the meristematic zone—although they failed to expand appreciably—developed characteristics of the cortex, including a central vacuole and a peripheral nuclear position (Figures 5 and 6). These characteristics differ qualitatively from the effects of both the *knolle* mutation and brefeldin A (see above). Thus, it appears that Sp2 expression not only affected cell expansion but also overruled the mechanism(s) holding the cells in an undifferentiated state, which permitted cell division to continue down the cell files.

How might the Sp2 peptide effect a block of secretion? The N-terminal region of t-SNAREs, such as syntaxin 1A and the yeast plasma membrane syntaxins Sso1 and Sso2, is now recognized to form an independently folded regulatory domain that includes the first three coiled-coil sequences (Jahn and Sudhof, 1999). This regulatory domain interacts with the syntaxin signature sequence to form a "closed state" (Fiebig et al., 1999; Misura et al., 2000) and probably contributes to controlled activation of the syntaxin (Misura et al., 2000). Computer-assisted analysis has predicted a similar folding for the N terminus for NtSyr1 (Blatt et al., 1999). Therefore, it is conceivable that, by introducing an excess of Sp2 (which includes this domain), NtSyr1 could be trapped in an equivalent closed conformation through direct binding with Sp2, preventing further SNARE interactions. The Sp2 peptide also contains the syntaxin signature sequence, which, in neuronal cells, interacts with domains of SNAP-25 and synaptobrevin to form the ternary SNARE complex. Thus, another explanation is that Sp2 interacts with the partners of NtSyr1, preventing them from building a functional SNARE complex (Hayashi et al., 1995; O'Connor et al., 1997; Ferrer Montiel et al., 1998; O'Sullivan et al., 1999; Scales et al., 2000). At present, our data do not allow us to discriminate between these alternatives. However, both explanations predict a dependence on the relative abundance of NtSyr1 and competing Sp2 peptide, a prediction that finds support in both the correlations between Sp2 expression and transgenic phenotype and the fact that Sp2 action could be overcome by increasing the level of NtSyr1 expression.

Relating NtSyr1 Actions in Membrane Traffic and Abscisic Acid–Mediated Ion Channel Control

The actions of the Sp2 peptide and of NtSyr1 overexpression on growth and secretion raise questions about their relationship to abscisic acid and the control of K^+ and Cl^- channels at the plasma membrane. Previously, we found that the Sp2 peptide and *Clostridium* BotN/C neurotoxin, which cleaves NtSyr1, each suppressed abscisic acid–evoked changes in the activities of three distinct ion channels in guard cells, and we suggested a role for NtSyr1 in their control on the basis of these observations (Leyman et al., 1999). Could the effects of Sp2 on control of the channels be explained as a consequence of its inhibition of vesicle (and membrane protein) traffic at the plasma membrane? Is the action of NtSyr1 in guard cells different from its activity in other cell types? And what is the relationship between traffic directed toward the plasma membrane, its block by Sp2, and the action of abscisic acid in guard cells, which ultimately must promote endocytosis, and a net loss in plasma membrane surface area?

A definitive answer to the first question requires direct monitoring of the K^+ and Cl^- channel protein traffic. In principle, the effects of abscisic acid on these channels, and its inhibition by the Sp2 peptide, could be brought about through changes in vesicle traffic at the guard cell plasma membrane. This explanation would accord with evidence linking trafficking and activity of mammalian epithelial Na^+ channels (Qi et al., 1999) and H^+-ATPase (Banerjee et al., 1999). Alternatively, NtSyr1 might play a more intimate role in abscisic acid signaling beyond the mechanics of vesicle trafficking, either through direct interactions with these channels (Stanley and Mirotznik, 1997; Naren et al., 1997, 1998; Bezprozvanny et al., 2000; Fili et al., 2001) or in scaffolding and nucleation of receptor-effector protein complexes (Fujita et al., 1998; Nishimune et al., 1998; Springer and Schekman, 1998; Hibino et al., 2000) that are essential features of many signaling cascades.

In fact, it is difficult to reconcile a single mechanism of action for abscisic acid mediated by vesicle traffic with the body of evidence for channel control mediated separately for each channel type by changes in $[Ca^{2+}]_i$, pH, and/or protein (de-)phosphorylation (MacRobbie, 1983; Ward et al., 1995; Thiel and Wolf, 1997; Blatt, 2000). An additional complication is that abscisic acid triggers opposing changes in the activity of two different classes of K^+ channels as well as activating Cl^- channels, and the effects of abscisic acid on the channel currents include changes in channel-gating properties that would imply selective addition and removal of subsets of channel proteins within each of these classes. Furthermore, the responses of at least two of these channels are complete within 1 to 2 min of exposure to abscisic acid, an order of magnitude faster than the onset for changes in cell volume, surface area, and stomatal closure. Consequently, it would be intriguing if the effects of Sp2 and *Clostridium* BotN/C neurotoxin on abscisic acid signaling in guard cells were mediated solely by the effects on membrane traffic, because this would suggest processes of membrane protein traffic that are rapid, highly targeted, and separate from the bulk flux of membrane that must accompany the changes in cell volume and surface area during stomatal closure. It also would imply that at least one membrane-trafficking step is a prerequisite for all of the other signaling pathways that may modulate ion channel activity at the plasma membrane. If NtSyr1 carries out additional functions specific to guard cells and associated aerial organs—a possibility given the differences in NtSyr1 expression patterns within the plant (Leyman et al., 2000)—the effect of abscisic acid might be to affect ion channel activity in part through changes in specialized trafficking pathways, perhaps altering the rate of recruitment of particular channels in guard cells.

Of the final question, the juxtaposed roles for NtSyr1 in traffic at the plasma membrane and in abscisic acid action that leads to a net reduction in plasma membrane surface area, presumably via endocytosis, we have noted already that the effects of Sp2 and NtSyr1 on secGFP and *N*-secYFPΔC secretion could be mediated at steps either in transport from the Golgi to the plasma membrane or in recycling and recovery of an essential membrane component (see above). The tools available simply cannot distinguish between these two mechanisms of action. It is possible that the bulk reduction in plasma membrane surface area during stomatal closure is mediated by trafficking events that use other SNARE molecules. However, if NtSyr1 contributed directly to endocytosis, and its block led to a subsequent reduction in forward traffic to the plasma membrane, it would resolve the apparent paradox of the requirement for NtSyr1 in normal secGFP export while still linking its role in abscisic acid–mediated stomatal closure with net endocytosis. The different time scales of the ion channel activity assays (Leyman et al., 1999) and the secGFP accumulation assays used here are consistent with this interpretation. Alternatively, it also is plausible that the SNARE protein could be an integral part of the mechanisms for both vesicle fusion at the final stages of trafficking to the plasma membrane and as a target element or regulator of nucleation as vesicles form at the onset of endocytosis from the plasma membrane (Jarousse and Kelly, 2001). Again, an answer requires direct, unidirectional monitoring of protein traffic at the cell surface.

METHODS

Plant Growth and Protocols

Tobacco (*Nicotiana tabacum* cv SR1) transformed with *Agrobacterium tumefaciens* LBA4404 carrying various constructs (see below) was grown in a greenhouse at 25°C and scored for Sp1 and Sp2 expression by immunochemical analysis. T-DNA insertions were verified by DNA gel blot analysis (Sambrook et al., 1989) using radiolabeled *NtSyr1* cDNA as a probe. Positive lines were crossed with themselves, and seed of the T1 and later generations were used for experimental analysis.

For experiments with mature *dexSp2* transgenic tobacco, the plants were sprayed and watered as indicated in text with a solution of 20 μM dexamethasone (cyclodextrin encapsulated; Sigma, Poole, UK). The expression of Sp2 was characterized in detail in three lines, *dexSp2-10*, *dexSp2-16*, and *dexSp2-14*, that gave moderate, low, and high levels of Sp2 expression, respectively. For these experiments, 100 seed were sterilized by treating them with a 10 to 13% $NaClO_3$ solution for 10 min, rinsed five times in sterile, distilled water, and stored overnight at 4°C. The seed then were incubated in 100 mL of sterile Murashige and Skoog (1962) (MS) medium with 10 mM Mes buffer, pH 5.7, on a rotary shaker (120 rpm) under 60 $\mu mol \cdot m^{-2} \cdot sec^{-1}$ fluorescent light at 25°C. For growth in dexamethasone, the steroid was added to give a final concentration of 20 μM stock solution.

35S-Sp1, 35S-Sp2, and Dex-Sp2 Constructs

Histidine-tagged Sp1 and Sp2 constructs were generated by insertion of polymerase chain reaction–amplified DNA fragments in the plasmid pQE30 (Qiagen, Crawley, UK). The common forward primer was 5′-GCGGATCCATGAATGATCTATTTT-3′, and the reverse primers were 5′-GCCTGCAGTCATTTTTTTCCATGGC-3′ for amplification of the Sp1 DNA fragment and 5′-GCCTGCAGTTAACAAGTCCATTTT-3′ for amplification of the Sp2 DNA fragment. A 35S promoter was inserted upstream in each case, using the EcoRI site of pQE30. DNA fragments comprising the 35S promoter and histidine-tagged Sp1 or Sp2 were cloned subsequently as a HindIII fragment in the binary vector pCAMBIA1380. For inducible expression, the Sp2 gene was cloned into pBSKS (New England Biolabs, Hitchin, UK) and subsequently as a SpeI–SalI DNA fragment inserted into the vector pTA7002 containing the two-component glucocorticoid-inducible system (Aoyama and Chua, 1997). All constructs were checked by sequencing.

Root Growth Measurements

Plants were grown under sterile conditions in 12-cm^2 Petri dishes with 45 mL of MS medium in 0.7% (w/v) Phytagel (Sigma). Seed were sown at 1-cm intervals, two rows per plate, and were grown with the plates on end under 500 μmol · m^{-2} · sec^{-1} PAR light in a 16-hr/8-hr light/dark cycle at 21°C. For *dexSp2* induction, 1 μM dexamethasone was included in the medium. Plates were photographed at 24-hr intervals for subsequent measurements of root growth. Growth inhibition was determined either as the difference in mean root length between plants grown on MS medium compared with plants grown on MS medium containing 1 μM dexamethasone or as the corresponding ratio of the mean rates of growth 3 days after germination.

Immunodetection of NtSyr1 and Related Constructs

Crude protein was extracted by grinding tissue frozen in liquid nitrogen. The powdered material was resuspended 1:1 (w/v) in extraction buffer containing 100 mM Tris-HCl, pH 8.0, 1% SDS, 1% sodium deoxycholate, 20 mM EDTA, 1 mM DTT, and 0.2 mM phenylmethylsulfonyl fluoride. Each sample was centrifuged at 10,000*g* for 10 min at 4°C, and the supernatant was collected. SDS was removed by centrifugation at 16,000*g* for 3 min after mixing with 20 volumes of 100 mM KH_2PO_4. Protein was quantified by Bradford assay (Bio-Rad, Hemel Hampstead, UK) and calibrated against BSA.

Membrane proteins were extracted by resuspension of ground tissue in extraction buffer containing 100 mM Tris-Cl, pH 7.5, 300 mM sucrose, 1 mM EDTA, 2.5 mM DTT, and 0.1 mM phenylmethylsulfonyl fluoride. Each sample was homogenized in a potter and centrifuged at 10,000*g* at 4°C. The supernatant was collected, and the microsome membrane fraction was pelleted by centrifugation at 50,000*g* for 35 min at 4°C. Proteins were separated by SDS-PAGE and transferred to a nitrocellulose membrane using an electrophoretic transfer cell (Bio-Rad), according to the manufacturer's specifications. NtSyr1 and NtSyr1 peptides were detected with a rabbit polyclonal antiserum (1:2000 dilution) as described previously (Leyman et al., 1999, 2000). Histidine tags were detected with a mouse anti-RGS(H)$_4$ monoclonal antibody (1:1000 dilution; Qiagen) and a secondary rabbit anti-mouse antibody labeled with alkaline phosphatase. Substrates were nitroblue tetrazolium and 5-bromo-4-chloro-3-indolyl phosphate (Sigma).

Histochemistry and Microscopy

Tissues were sectioned after fixing in 50 mM cacodylate buffer, pH 7.2, with 2.5% glutaraldehyde at 4°C. After 24 hr, samples were washed twice in the same buffer minus glutaraldehyde, postfixed with 2% OsO_4 in the same buffer for 90 min, and finally washed twice for 10 min in cacodylate buffer and then water. Tissues were dehydrated through an acetone/water series followed by three washes with 100% acetone and were embedded in Epon-araldite resin in progressive steps of acetone/resin mixture, first 4:1 (4 hr), 2:1 (4 hr), 1:1 (10 hr), 1:2 (10 hr), 1:4 (12 hr), and three subsequent steps in pure resin (12 hr). Samples were placed in molds with fresh resin and polymerized at 60°C for 48 hr. Blocks were cut with a glass knife, and sections were mounted and stained with 0.1% toluene blue.

Transient Expression and Analysis of Green Fluorescent Protein and Yellow Fluorescent Protein Secretion with Nt-Syr1 Constructs

Plasmids pVKH-*N*-ST-green fluorescent protein (GFP), pVKH-GFP-HDEL, and pVKH-secGFP encoding the Golgi-targeted *N*-ST-GFP, endoplasmic reticulum (ER)–targeted GFP-HDEL, and secreted secGFP, respectively, are described elsewhere (Batoko et al., 2000). The yellow fluorescent protein (YFP) variant of *N*-secGFP was constructed by amplifying the chitinase signal peptide and synthetic N-glycosylated peptide exactly as described for *N*-secGFP (Batoko et al., 2000) and inserting it as an XbaI–XhoI fragment into the XbaI and SalI sites upstream of YFP in the plasmid pVKH-*N*-ST-YFP (a gift of Dr. F. Branizzi, Oxford-Brookes University, Oxford, UK) to generate pVKH-*N*-secYFP. The primers nsec-YFPΔC-5′ (5′-AGCCGT AGCGCTCGAGCGCGCGTATTTTTACAACAAT-3′) and nsec-YFPΔC-3′ (5′-AACGATTCAACATCTTTAGGCGGCGGTCACGAACTCC-3′) were used in conjunction with pVKH-*N*-secYFP to generate a fragment by polymerase chain reaction containing the tobacco mosaic virus Ω translation initiation enhancer and a YFP coding region in which the last 11 amino acids were replaced by a stop codon. This fragment was digested by XhoI and BglII and cloned into XhoI–BamHI downstream of the 35S promoter in the expression cassette of pK1102, a derivative of pRT101 (Topfer et al., 1987). This expression cassette was subcloned into the binary vector pGREEN (Hellens et al., 2000) as a HindIII fragment to generate pG-N-secYFPΔC, which was introduced by electroporation into *A. tumefaciens* GV3101::pMP90 (Koncz and Schell, 1986) containing pSoup, which is required for replication of pGREEN in *A. tumefaciens*. Transient expression of these constructs has been described (Batoko et al., 2000).

For experiments with dexSp2 transgenic tobacco, the secGFP-containing strain (final $OD_{600} = 0.01$) was resuspended in the infiltration buffer with or without dexamethasone to induce expression of the Sp2 fragment. For coexpression experiments, all strains were inoculated at $OD_{600} = 0.1$. Expression of fluorescence in epidermal cells of the lower epidermis was assessed 2 to 3 days after infiltration. Pieces of leaf were sampled randomly from the infected area and mounted in water for observation under the microscope. In experiments with GFP alone (Figure 9), a Zeiss (Jena, Germany) CLSM410 confocal microscope was used with samples mounted in water or 30 μM propidium iodide to label the apoplast. Double-labeling experiments were performed on a Zeiss CLSM510 confocal microscope using the 458- and 514-nm lines from a 25-mW argon laser set at 75% and an HFT 458/514 dichroic mirror. An NFT 515 dichroic was used to split the emitted light between channels set (1) with a 204-μm pinhole and 475- to 525-nm bandpass filter for GFP detection, and (2) with a 213-μm pinhole and 535- to 590-nm infrared bandpass filter to detect YFP. For the images in Figures 10K to 10T, track 1 was configured with detector gains of 910 and 0 V in the GFP and YFP channels, respectively, with the 458-nm laser line attenuated to 21% and the 514-nm line attenuated fully; track 2 was configured with detector gains of 0 and 970 V in the GFP and YFP channels, respectively, with the 458-nm line attenuated fully and the 514-nm line attenuated to 4%.

ACKNOWLEDGMENTS

We thank John Haines and Nina Grabov for technical and photographic support, Lauren Hughes for help with root growth measurements, and Ian Brown for his comments on microscopic analysis. Maren Heese and Gerd Jürgens provided helpful comments on the manuscript. This work was supported by the Biotechnology and Biological Science Research Council (H.B. and I.M.) and by a grant-in-aid from the Gatsby Charitable Foundation, European Union Biotech Grant No. CT96-0062, Biotechnology and

Biological Science Research Council Grant Nos. P08406 and P012750, and Human Frontier Science Program Grant No. RG303/95M (D.G., B.L., G.-P.D.S., and M.R.B.).

Received August 3, 2001; accepted October 23, 2001.

REFERENCES

Aalto, M.K., Ronne, H., and Keranen, S. (1993). Yeast syntaxins sso1p and sso2p belong to a family of related membrane-proteins that function in vesicular transport. EMBO J. **12,** 4095–4104.

Aoyama, T., and Chua, N.H. (1997). A glucocorticoid-mediated transcriptional induction system in transgenic plants. Plant J. **11,** 605–612.

Avery, J., Jahn, R., and Edwardson, J.M. (1999). Reconstitution of regulated exocytosis in cell-free systems: A critical appraisal. Annu. Rev. Physiol. **61,** 777–807.

Banerjee, A., Shih, T., Alexander, E.A., and Schwartz, J.H. (1999). SNARE proteins regulate H^+-ATPase redistribution to the apical membrane in rat renal inner medullary collecting duct cells. J. Biol. Chem. **274,** 26518–26522.

Baskin, T.I., and Bivens, N.J. (1995). Stimulation of radial expansion in *Arabidopsis* roots by inhibitors of actomyosin and vesicle secretion but not by various inhibitors of metabolism. Planta **197,** 514–521.

Bassham, D.C., and Raikhel, N.V. (1999). The pre-vacuolar t-SNARE AtPEP12p forms a 20S complex that dissociates in the presence of ATP. Plant J. **19,** 599–603.

Batoko, H., Zheng, H.Q., Hawes, C., and Moore, I. (2000). A Rab1 GTPase is required for transport between the endoplasmic reticulum and Golgi apparatus and for normal Golgi movement in plants. Plant Cell **12,** 2201–2217.

Battey, N.H., and Blackbourn, H.D. (1993). The control of exocytosis in plant cells. New Phytol. **125,** 307–338.

Battey, N., Carroll, A., Vankesteren, R., Taylor, A., and Brownlee, C. (1996). The measurement of exocytosis in plant cells. J. Exp. Bot. **47,** 717–728.

Battey, N.H., James, N.C., Greenland, A.J., and Brownlee, C. (1999). Exocytosis and endocytosis. Plant Cell **11,** 643–659.

Bennett, M.K., Garciaarraras, J.E., Elferink, L.A., Peterson, K., Fleming, A.M., Hazuka, C.D., and Scheller, R.H. (1993). The syntaxin family of vesicular transport receptors. Cell **74,** 863–873.

Bezprozvanny, I., Zhong, P.Y., Scheller, R.H., and Tsien, R.W. (2000). Molecular determinants of the functional interaction between syntaxin and N-type Ca^{2+} channel gating. Proc. Natl. Acad. Sci. USA **97,** 13943–13948.

Blatt, M.R. (2000). Cellular signaling and volume control in stomatal movements in plants. Annu. Rev. Cell Dev. Biol. **16,** 221–241.

Blatt, M.R., Leyman, B., and Geelen, D. (1999). Molecular events of vesicle trafficking and control by SNARE proteins in plants. New Phytol. **144,** 389–418.

Boevink, P., Oparka, K., Cruz, S.S., Martin, B., Betteridge, A., and Hawes, C. (1998). Stacks on tracks: The plant Golgi apparatus traffics on an actin/ER network. Plant J. **15,** 441–447.

Boevink, P., Martin, B., Oparka, K., Cruz, S.S., and Hawes, C. (1999). Transport of virally expressed green fluorescent protein through the secretory pathway in tobacco leaves is inhibited by cold shock and brefeldin A. Planta **208,** 392–400.

Carroll, A.D., Moyen, C., VanKesteren, P., Tooke, F., Battey, N.H., and Brownlee, C. (1998). Ca^{2+}, annexins, and GTP modulate exocytosis from maize root cap protoplasts. Plant Cell **10,** 1267–1276.

Conceicao, A.S., Marty Mazars, D., Bassham, D.C., Sanderfoot, A.A., Marty, F., and Raikhel, N.V. (1997). The syntaxin homolog AtPEP12p resides on a late post-Golgi compartment in plants. Plant Cell **9,** 571–582.

Degtiar, V.E., Scheller, R.H., and Tsien, R.W. (2000). Syntaxin modulation of slow inactivation of N-type calcium channels. J. Neurosci. **20,** 4355–4367.

Dolan, L., and Okada, K. (1999). Signalling in cell type specification. Semin. Cell Dev. Biol. **10,** 149–156.

Dolan, L., and Roberts, K. (1995). 2 ways to skin a plant: The analysis of root and shoot epidermal development in *Arabidopsis*. BioEssays **17,** 865–872.

Fasshauer, D., Antonin, W., Margittai, M., Pabst, S., and Jahn, R. (1999). Mixed and non-cognate SNARE complexes: Characterization of assembly and biophysical properties. J. Biol. Chem. **274,** 15440–15446.

Ferrer Montiel, A.V., Gutierrez, L.M., Apland, J.P., Canaves, J.M., Gil, A., Viniegra, S., Biser, J.A., Adler, M., and Montal, M. (1998). The 26-mer peptide released from SNAP-25 cleavage by botulinum neurotoxin E inhibits vesicle docking. FEBS Lett. **435,** 84–88.

Fiebig, K.M., Rice, L.M., Pollock, E., and Brunger, A.T. (1999). Folding intermediates of SNARE complex assembly. Nat. Struct. Biol. **6,** 117–123.

Fili, O., Michaelevski, I., Bledi, Y., Chikvashvili, D., Singer-Lahat, D., Boshwitz, H., Linial, M., and Lotan, I. (2001). Direct interaction of a brain voltage-gated K^+ channel with syntaxin 1A: Functional impact on channel gating. J. Neurosci. **21,** 1964–1974.

Fujita, Y., Shirataki, H., Sakisaka, T., Asakura, T., Ohya, T., Kotani, H., Yokoyama, S., Nishioka, H., Matsuura, Y., Mizoguchi, A., Scheller, R.H., and Takai, Y. (1998). Tomosyn: A syntaxin-1-binding protein that forms a novel complex in the neurotransmitter release process. Neuron **20,** 905–915.

Fukuda, R., Mcnew, J.A., Weber, T., Parlati, F., Engel, T., Nickel, W., Rothman, J.E., and Sollner, T.H. (2000). Functional architecture of an intracellular membrane t-SNARE. Nature **407,** 198–202.

Hanson, P.I., Heuser, J.E., and Jahn, R. (1997). Neurotransmitter release: Four years of SNARE complexes. Curr. Opin. Neurobiol. **7,** 310–315.

Hayashi, T., Yamasaki, S., Nauenburg, S., Binz, T., and Niemann, H. (1995). Disassembly of the reconstituted synaptic vesicle membrane fusion complex in vitro. EMBO J. **14,** 2317–2325.

Hellens, R.P., Edwards, E.A., Leyland, N.R., Bean, S., and Mullineaux, P.M. (2000). pGreen: A versatile and flexible binary Ti vector for *Agrobacterium*-mediated plant transformation. Plant Mol. Biol. **42,** 819–832.

Hibino, H., Inanobe, A., Tanemoto, M., Fujita, A., Doi, K., Kubo, T., Hata, Y., Takai, Y., and Kurachi, Y. (2000). Anchoring proteins confer G protein sensitivity to an inward-rectifier K^+ channel through the GK domain. EMBO J. **19,** 78–83.

Holthuis, J.C.M., Nichols, B.J., Dhruvakumar, S., and Pelham, H.R.B. (1998). Two syntaxin homologues in the TGN/endosomal system of yeast. EMBO J. **17,** 113–126.

Homann, U., and Tester, M. (1997). Ca^{2+}-independent and Ca^{2+}/GTP-binding protein-controlled exocytosis in a plant cell. Proc. Natl. Acad. Sci. USA **94,** 6565–6570.

Jahn, R., and Sudhof, T.C. (1999). Membrane fusion and exocytosis. Annu. Rev. Biochem. **68,** 863–911.

Jarousse, N., and Kelly, R.B. (2001). The AP2 binding site of synaptotagmin 1 is not an internalization signal but a regulator of endocytosis. J. Cell Biol. **154,** 857–866.

Jin, J.B., Kim, Y.A., Kim, S.J., Lee, S.H., Kim, D.H., Cheong, G.W., and Hwang, I. (2001). A new dynamin-like protein, ADL6, is involved in trafficking from the *trans*-Golgi network to the central vacuole in *Arabidopsis*. Plant Cell **13,** 1511–1525.

Jones, J.D.G., Shulumukov, L., Carland, F., English, J.J., Scofield, S.R., Bishop, G.J., and Harrison, K. (1992). Effective vectors for transformation, expression of heterologous genes, and assaying transposon excision in transgenic plants. Transgenic Res. **1,** 285–297.

Kaiser, C.A., Gimeno, R.E., and Shaywitz, D.A. (1997). Protein secretion, membrane biogenesis and endocytosis. In The Molecular and Cellular Biology of the Yeast *Saccharomyces*, J.R. Pringle, J.R. Broach, and E.W. Jones, eds (Cold Spring Harbor, NY: Cold Spring Harbor Laboratory Press), pp. 91–227.

Kang, H.G., Fang, Y.W., and Singh, K.B. (1999). A glucocorticoid-inducible transcription system causes severe growth defects in *Arabidopsis* and induces defense-related genes. Plant J. **20,** 127–133.

Koncz, C., and Schell, J. (1986). The promoter of TL-DNA gene 5 controls the tissue-specific expression of chimeric genes carried by a novel type of *Agrobacterium* binary vector. Mol. Gen. Genet. **204,** 383–396.

Kunze, I., Hillmer, S., Kunze, G., and Muntz, K. (1995). Brefeldin A differentially affects protein secretion from suspension-cultured tobacco cells (*Nicotiana tabacum* L.). J. Plant Physiol. **146,** 71–80.

Lauber, M.H., Waizenegger, I., Steinmann, T., Schwarz, H., Mayer, U., Hwang, I., Lukowitz, W., and Jurgens, G. (1997). The Arabidopsis KNOLLE protein is a cytokinesis-specific syntaxin. J. Cell Biol. **139,** 1485–1493.

Leyman, B., Geelen, D., Quintero, F.J., and Blatt, M.R. (1999). A tobacco syntaxin with a role in hormonal control of guard cell ion channels. Science **283,** 537–540.

Leyman, B., Geelen, D., and Blatt, M.R. (2000). Localization and control of expression of Nt-Syr1, a tobacco SNARE protein. Plant J. **24,** 369–381.

Lukowitz, W., Mayer, U., and Jurgens, G. (1996). Cytokinesis in the *Arabidopsis* embryo involves the syntaxin related *knolle* gene product. Cell **84,** 61–71.

MacRobbie, E.A.C. (1983). Ionic relations of stomatal guard cells. In Stomatal Physiology, P.E. Jarvis and T.A. Mansfield, eds (Cambridge, UK: Cambridge University Press), pp. 52–70.

Mayer, R.J., and Marshall, L.A. (1993). New insights on mammalian phospholipase A_2(s): Comparison of arachidonoyl-selective and -nonselective enzymes. FASEB J. **7,** 339–348.

McNellis, T.W., Mudgett, M.B., Li, K., Aoyama, T., Horvath, D., Chua, N.H., and Staskawicz, B.J. (1998). Glucocorticoid-inducible expression of a bacterial avirulence gene in transgenic *Arabidopsis* induces hypersensitive cell death. Plant J. **14,** 247–257.

Mcnew, J.A., Parlati, F., Fukuda, R., Johnston, R.J., Paz, K., Paumet, F., Sollner, T.H., and Rothman, J.E. (2000). Compartmental specificity of cellular membrane fusion encoded in SNARE proteins. Nature **407,** 153–159.

Misura, K.M.S., Scheller, R.H., and Weis, W.I. (2000). Three-dimensional structure of the neuronal-Sec1-syntaxin 1a complex. Nature **404,** 355–362.

Morris, D.A., and Robinson, J.S. (1998). Targeting of auxin carriers to the plasma membrane: Differential effects of brefeldin A on the traffic of auxin uptake and efflux carriers. Planta **205,** 606–612.

Murashige, T., and Skoog, F. (1962). A revised medium for rapid growth and bioassays with tobacco tissue culture. Physiol. Plant. **15,** 473–497.

Naren, A.P., Nelson, D.J., Xie, W.W., Jovov, B., Pevsner, J., Bennett, M.K., Benos, D.J., Quick, M.W., and Kirk, K.L. (1997). Regulation of CFTR chloride channels by syntaxin and Munc18 isoforms. Nature **390,** 302–305.

Naren, A.P., Quick, M.W., Collawn, J.F., Nelson, D.J., and Kirk, K.L. (1998). Syntaxin 1A inhibits CFTR chloride channels by means of domain-specific protein-protein interactions. Proc. Natl. Acad. Sci. USA **95,** 10972–10977.

Nichols, B.J., and Pelham, H.R.B. (1998). SNAREs and membrane fusion in the Golgi apparatus. Biochim. Biophys. Acta **1404,** 9–31.

Nickel, W., Weber, T., Mcnew, J.A., Parlati, F., Sollner, T.H., and Rothman, J.E. (1999). Content mixing and membrane integrity during membrane fusion driven by pairing of isolated v-SNAREs and t-SNAREs. Proc. Natl. Acad. Sci. USA **96,** 12571–12576.

Nishimune, A., Isaac, J.T.R., Molnar, E., Noel, J., Nash, S.R., Tagaya, M., Collingridge, G.L., Nakanishi, S., and Henley, J.M. (1998). NSF binding to GluR2 regulates synaptic transmission. Neuron **21,** 87–97.

O'Connor, V., Heuss, C., DeBello, W.M., Dresbach, T., Charlton, M.P., Hunt, J.H., Pellegrini, L.L., Hodel, A., Burger, M.M., Betz, H., Augustine, G.J., and Schafer, T. (1997). Disruption of syntaxin-mediated protein interactions blocks neurotransmitter secretion. Proc. Natl. Acad. Sci. USA **94,** 12186–12191.

O'Sullivan, G.A., Mohammed, N., Foran, P.G., Lawrence, G.W., and Dolly, J.O. (1999). Rescue of exocytosis in botulinum toxin A-poisoned chromaffin cells by expression of cleavage-resistant SNAP-25: Identification of the minimal essential C-terminal residues. J. Biol. Chem. **274,** 36897–36904.

Parlati, F., Weber, T., Mcnew, J.A., Westermann, B., Sollner, T.H., and Rothman, J.E. (1999). Rapid and efficient fusion of phospholipid vesicles by the α-helical core of a SNARE complex in the absence of an N-terminal regulatory domain. Proc. Natl. Acad. Sci. USA **96,** 12565–12570.

Parlati, F., Mcnew, J.A., Fukuda, R., Miller, R., Sollner, T.H., and Rothman, J.E. (2000). Topological restriction of SNARE-dependent membrane fusion. Nature **407,** 194–198.

Pfeffer, S.R. (1996). Transport vesicle docking: SNAREs and associates. Annu. Rev. Cell Dev. Biol. **12,** 441–461.

Qi, J.J., Peters, K.W., Liu, C.G., Wang, J.M., Edinger, R.S.,

Johnson, J.P., Watkins, S.C., and Frizzell, R.A. (1999). Regulation of the amiloride-sensitive epithelial sodium channel by syntaxin 1A. J. Biol. Chem. **274,** 30345–30348.

Rojo, E., Gillmor, C.S., Kovaleva, V., Somerville, C., and Raikhel, N.V. (2001). *VACUOLELESS1* is an essential gene required for vacuole formation in *Arabidopsis thaliana*. Dev. Cell **1,** 303–310.

Sambrook, J., Fritsch, E.F., and Maniatis, T. (1989). Molecular Cloning: A Laboratory Manual. (Cold Spring Harbor, NY: Cold Spring Harbor Laboratory Press).

Sanderfoot, A.A., and Raikhel, N.V. (1999). The specificity of vesicle trafficking: Coat proteins and SNAREs. Plant Cell **11,** 629–641.

Sanderfoot, A.A., Kovaleva, V., Zheng, H.Y., and Raikhel, N.V. (1999). The t-SNARE AtVAM3p resides on the prevacuolar compartment in *Arabidopsis* root cells. Plant Physiol. **121,** 929–938.

Sanderfoot, A.A., Assaad, F.F., and Raikhel, N.V. (2000). The *Arabidopsis* genome: An abundance of soluble *N*-ethylmaleimide-sensitive factor adaptor protein receptors. Plant Physiol. **124,** 1558–1569.

Sanderfoot, A.A., Pilgrim, M., Adam, L., and Raikhel, N.V. (2001). Disruption of individual members of *Arabidopsis* syntaxin gene families indicates each has essential functions. Plant Cell **13,** 659–666.

Satiat Jeunemaitre, B., Steele, C., and Hawes, C. (1996). Golgi-membrane dynamics are cytoskeleton dependent: A study on Golgi stack movement induced by brefeldin A. Protoplasma **191,** 21–33.

Sato, M.H., Nakamura, N., Ohsumi, Y., Kouchi, H., Kondo, M., Hara Nishimura, I., Nishimura, M., and Wada, Y. (1997). The AtVAM3 encodes a syntaxin-related molecule implicated in the vacuolar assembly in *Arabidopsis thaliana*. J. Biol. Chem. **272,** 24530–24535.

Scales, S.J., Chen, Y.A., Yoo, B.Y., Patel, S.M., Doung, Y.C., and Scheller, R.H. (2000). SNAREs contribute to the specificity of membrane fusion. Neuron **26,** 457–464.

Scheres, B., and Heidstra, R. (1999). Digging out roots: Pattern formation, cell division, and morphogenesis in plants. Curr. Top. Dev. Biol. **45,** 207–247.

Shevell, D.E., Leu, W.M., Gillmor, C.S., Xia, G.X., Feldmann, K.A., and Chua, N.H. (1994). Emb30 is essential for normal-cell division, cell expansion, and cell adhesion in Arabidopsis and encodes a protein that has similarity to sec7. Cell **77,** 1051–1062.

Springer, S., and Schekman, R. (1998). Nucleation of CopII vesicular coat complex by endoplasmic reticulum to Golgi vesicle SNAREs. Science **281,** 698–700.

Stanley, E.F., and Mirotznik, R.R. (1997). Cleavage of syntaxin prevents G-protein regulation of presynaptic calcium channels. Nature **385,** 340–343.

Steinmann, T., Geldner, N., Grebe, M., Mangold, S., Jackson, C.L., Paris, S., Galweiler, L., Palme, K., and Jurgens, G. (1999). Coordinated polar localization of auxin efflux carrier PIN1 by GNOM ARF GEF. Science **286,** 316–318.

Sutter, J.U., Homann, U., and Thiel, G. (2000). Ca^{2+}-stimulated exocytosis in maize coleoptile cells. Plant Cell **12,** 1127–1136.

Sutton, R.B., Fasshauer, D., Jahn, R., and Brunger, A.T. (1998). Crystal structure of a SNARE complex involved in synaptic exocytosis at 2.4 angstrom resolution. Nature **395,** 347–353.

Takeuchi, M., Ueda, T., Sato, K., Abe, H., Nagata, T., and Nakano, A. (2000). A dominant negative mutant of Sar1 GTPase inhibits protein transport from the endoplasmic reticulum to the Golgi apparatus in tobacco and *Arabidopsis* cultured cells. Plant J. **23,** 517–525.

Thiel, G., and Battey, N. (1998). Exocytosis in plants. Plant Mol. Biol. **38,** 111–125.

Thiel, G., and Wolf, A.H. (1997). Operation of K^+ channels in stomatal movement. Trends Plant Sci. **2,** 339–345.

Topfer, R., Matzeit, V., Gronenborn, B., Schell, J., and Steinbiss, H.H. (1987). A set of plant expression vectors for transcriptional and translational fusions. Nucleic Acids Res. **15,** 5890–5899.

von Mollard, G.F., and Stevens, T.H. (1999). The *Saccharomyces cerevisiae* v-SNARE Vti1p is required for multiple membrane transport pathways to the vacuole. Mol. Biol. Cell **10,** 1719–1732.

Ward, J.M., Pei, Z.M., and Schroeder, J.I. (1995). Roles of ion channels in initiation of signal transduction in higher plants. Plant Cell **7,** 833–844.

Weber, T., Zemelman, B.V., Mcnew, J.A., Westermann, B., Gmachl, M., Parlati, F., Sollner, T.H., and Rothman, J.E. (1998). SNAREpins: Minimal machinery for membrane fusion. Cell **92,** 759–772.

Wu, M.N., Fergestad, T., Lloyd, T.E., He, Y.C., Broadie, K., and Bellen, H.J. (1999). Syntaxin 1A interacts with multiple exocytic proteins to regulate neurotransmitter release in vivo. Neuron **23,** 593–605.

Yang, B., Gonzalez, L., Prekeris, R., Steegmaier, M., Advani, R.J., and Scheller, R.H. (1999). SNARE interactions are not selective: Implications for membrane fusion specificity. J. Biol. Chem. **274,** 5649–5653.

Zheng, H.Y., von Mollard, G.F., Kovaleva, V., Stevens, T.H., and Raikhel, N.V. (1999). The plant vesicle-associated SNARE AtVTI1a likely mediates vesicle transport from the *trans*-Golgi network to the prevacuolar compartment. Mol. Biol. Cell **10,** 2251–2264.